Additive Manufacturing of Metals and Alloys

7. Microstructure control through processing

February 2023

Dr. Charlotte de Formanoir
Prof. Roland Logé
MER Dr. Christian Leinenbach

EPFL

Introduction

In AM, there is limited margin for microstructure control through processing.

The process window is first dictated by the production of parts with the desired geometry and a minimal porosity content.

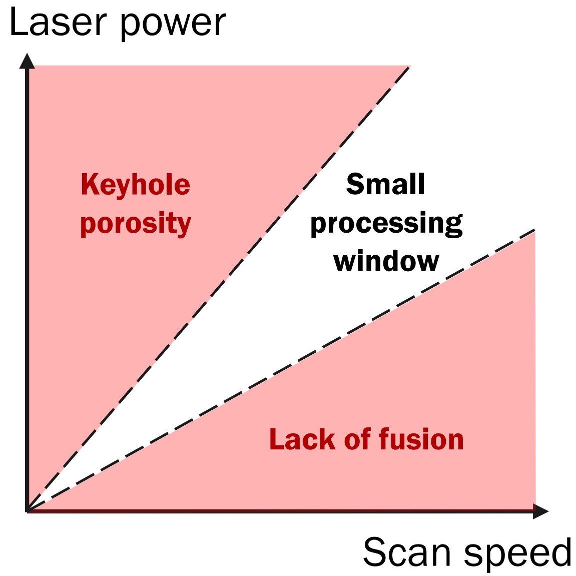

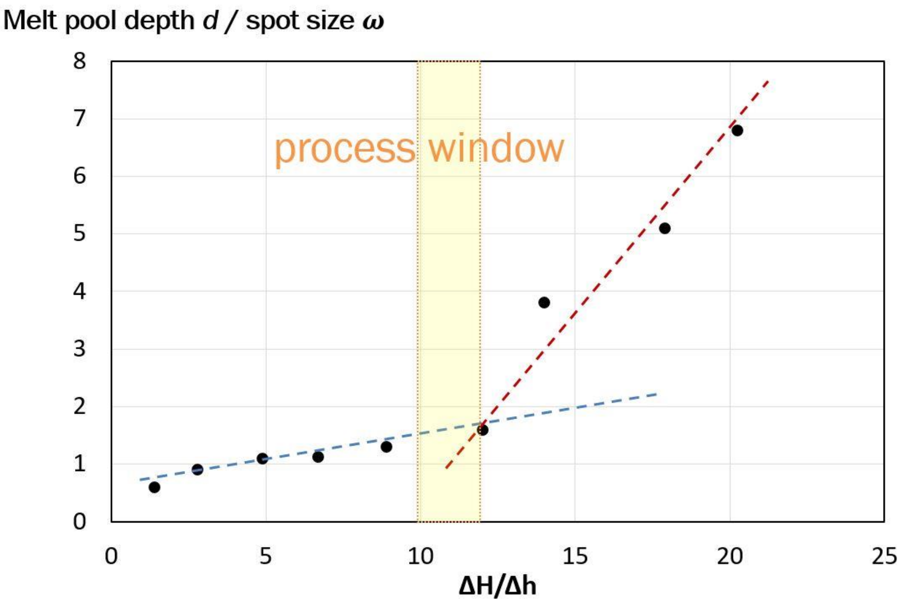

What are the options still available to control the microstructure during processing?

Microstructure control through processing

- Introduction: effect of thermal history on microstructure genesis
- Effect of scanning strategy
  - Effect of scanning direction
  - Effect of scanning length
- Effect of process parameters
- Effect of build geometry
- Effect of beamshaping
- Hybrid manufacturing
  - WAAM + rolling
  - LPBF + LSP

Microstructure control through processing

- Introduction: effect of thermal history on microstructure genesis
- Effect of scanning strategy
  - Effect of scanning direction
  - Effect of scanning length
- Effect of process parameters
- Effect of build geometry
- Effect of beamshaping
- Hybrid manufacturing
  - WAAM + rolling
  - LPBF + LSP

Introduction: effect of thermal history on microstructure genesis

Grain morphology

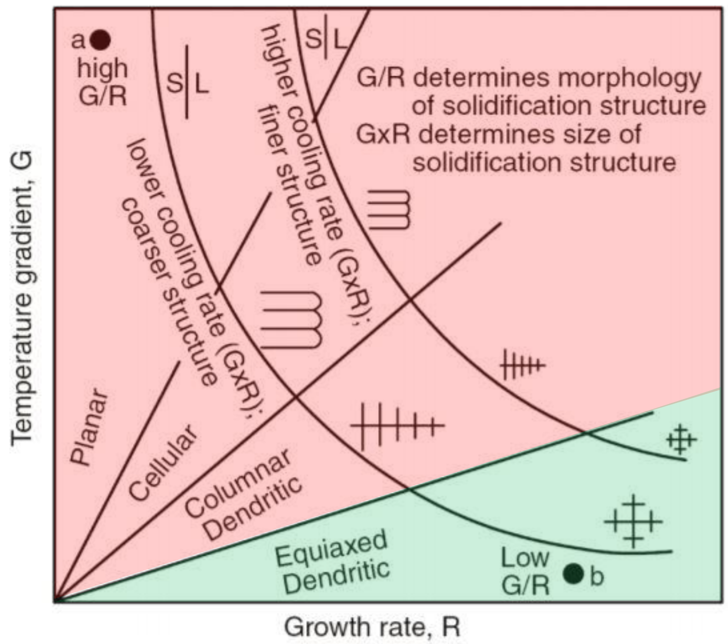

Columnar grains

Typically observed in AM (due to the very high temperature gradient on the order of 10^6 K/m)

Undesirable: <u>anisotropic</u> mechanical properties.

Equiaxed grains

Can be induced by:

- constitutional supercooling
- heterogeneous nucleation on partially melted powders
- heterogeneous nucleation on added refractory particles

Introduction: effect of thermal history on microstructure genesis

Grain size

Smaller grains are obtained by increasing the cooling rate GxR:
- low preheating temperature
- high scanning speed
- low power
- thin/small parts (low thermal mass)
- proximity to the build plate (= heat sink)

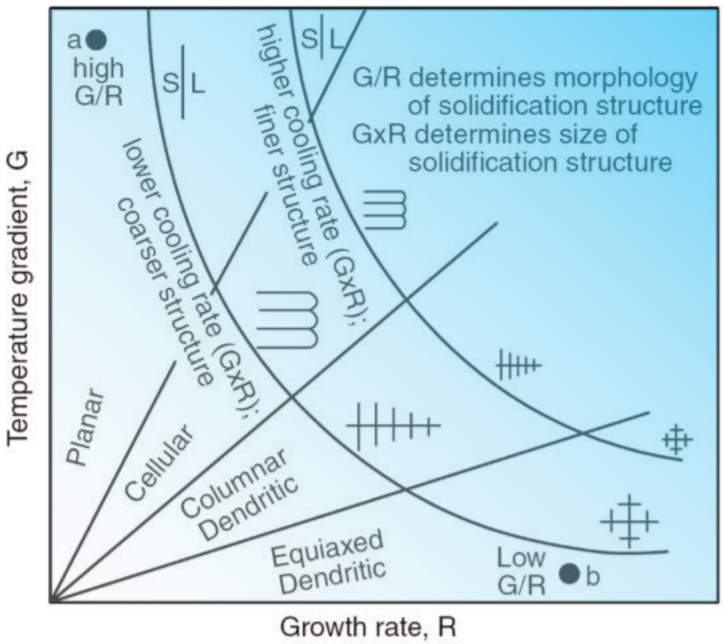

Microstructure control through processing

- Introduction: effect of thermal history on microstructure genesis
- Effect of scanning strategy
  - Effect of scanning direction
  - Effect of scanning length
- Effect of process parameters
- Effect of build geometry
- Effect of beamshaping
- Hybrid manufacturing
  - WAAM + rolling
  - LPBF + LSP

Effect of scanning strategy

Melt pool shape – DED vs PBF – longitudinal section

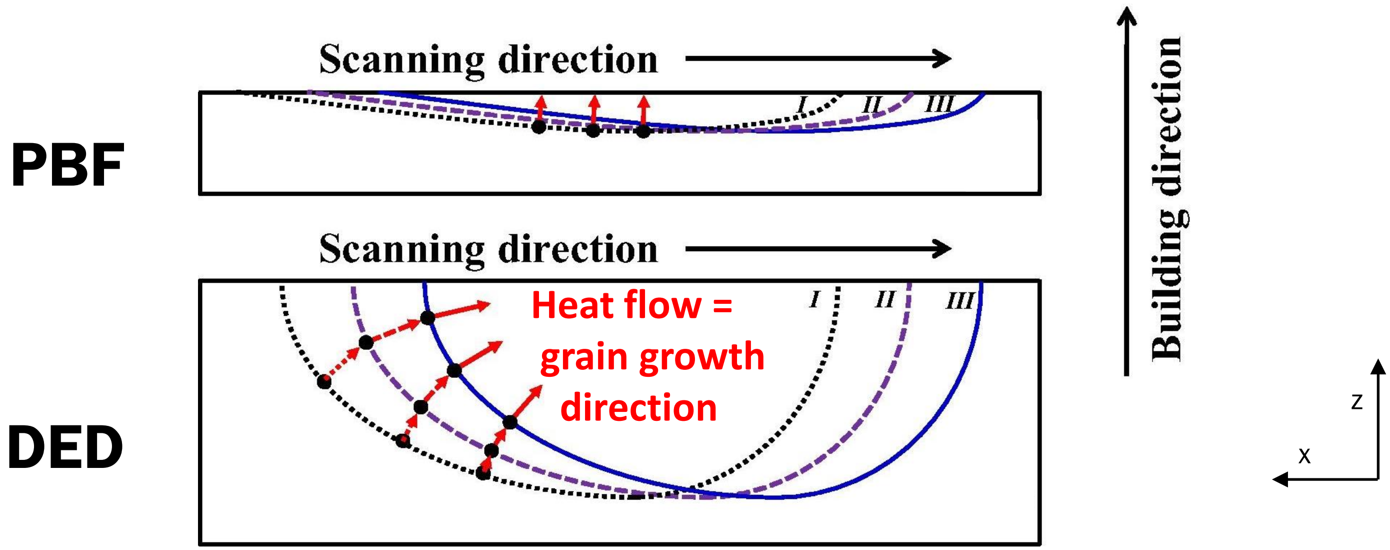

The orientation of the grain structure is affected by the shape and size of the melt pool.

The melt pool is long and shallow during PBF:
the heat flow at the melt pool boundary is opposite to the build direction.

The melt pool is short and deep during DED with a strong curvature:
the heat flow direction depends on the local position at the melt pool boundary.

DebRoy, Tarasankar, et al. "Additive manufacturing of metallic components–process, structure and properties." *Progress in Materials Science* 92 (2018): 112-224.

Ti64 – LPBF

Effect of scanning strategy

Unidirectional vs bidirectional – PBF – longitudinal section

In Ti64, β grains grow epitaxially, i.e. with the same crystallographic orientation as the already solidified material lying below.

The columnar grains are aligned with the maximum thermal gradient, i.e. perpendicular to the melt pool. Depending on the scanning direction and speed, the angle between the grain direction and the build orientation can vary.

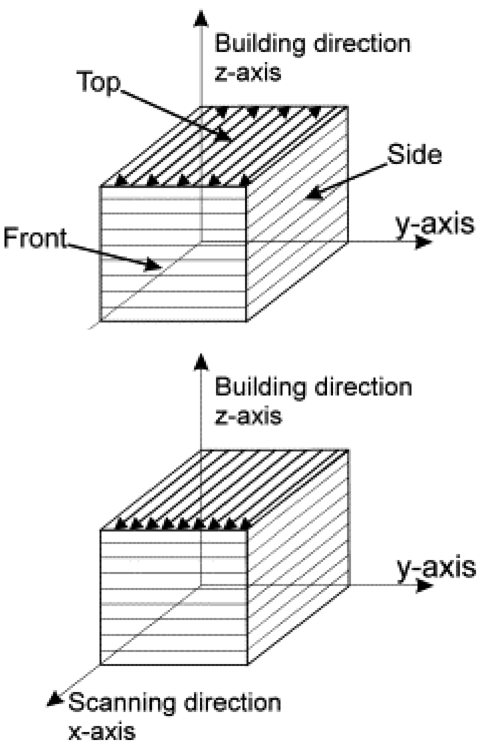

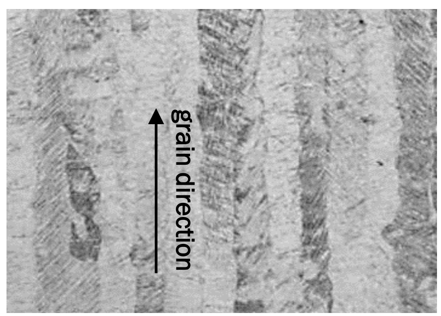

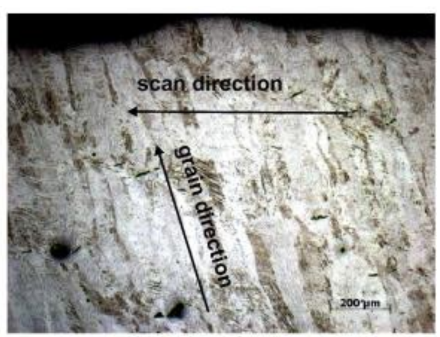

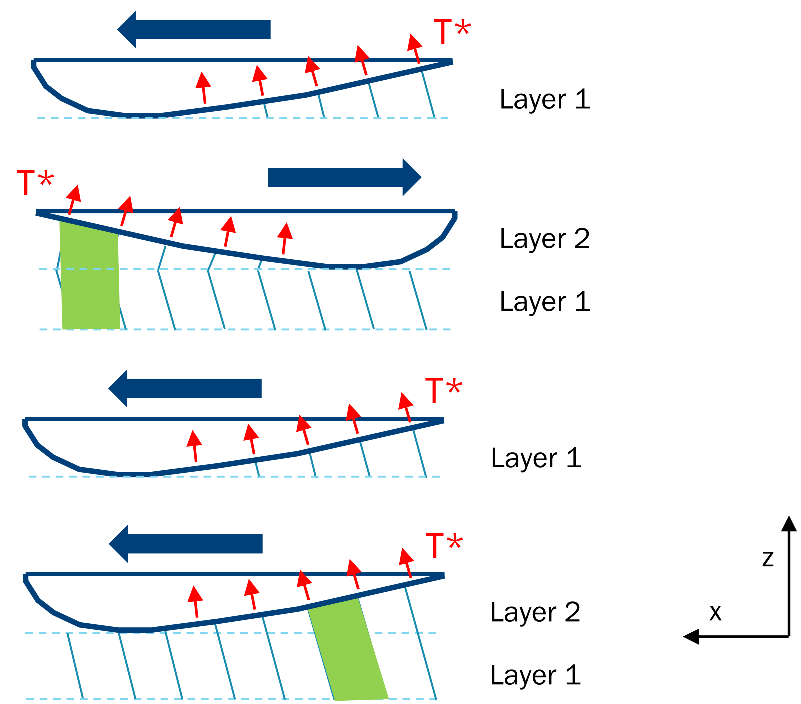

Thijs, Lore, et al. "A study of the microstructural evolution during selective laser melting of Ti–6Al–4V." *Acta materialia* 58.9 (2010): 3303-3312.

Effect of scanning strategy

Unidirectional vs bidirectional – DED

longitudinal section

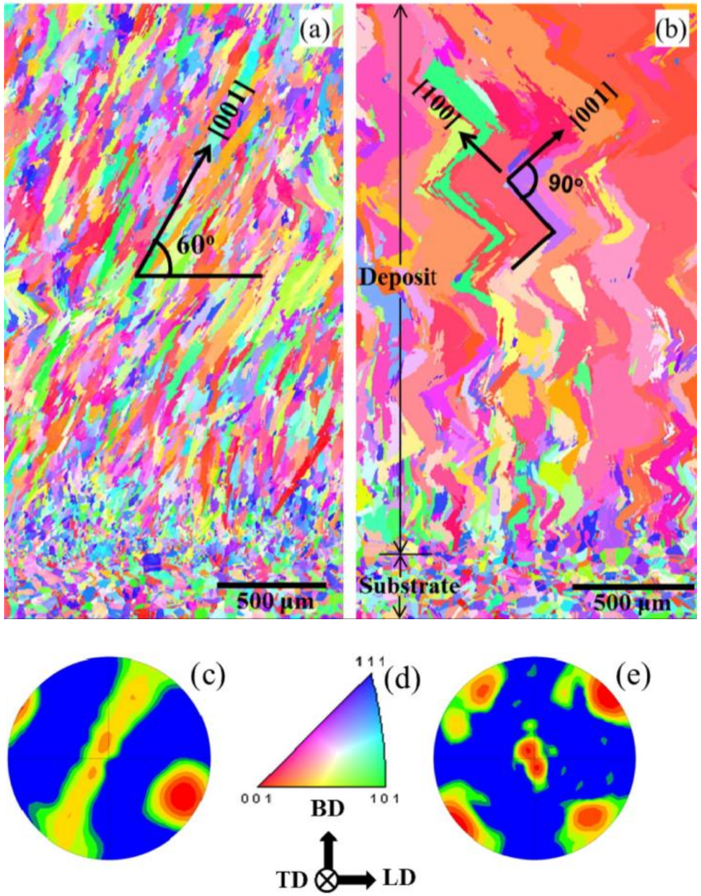

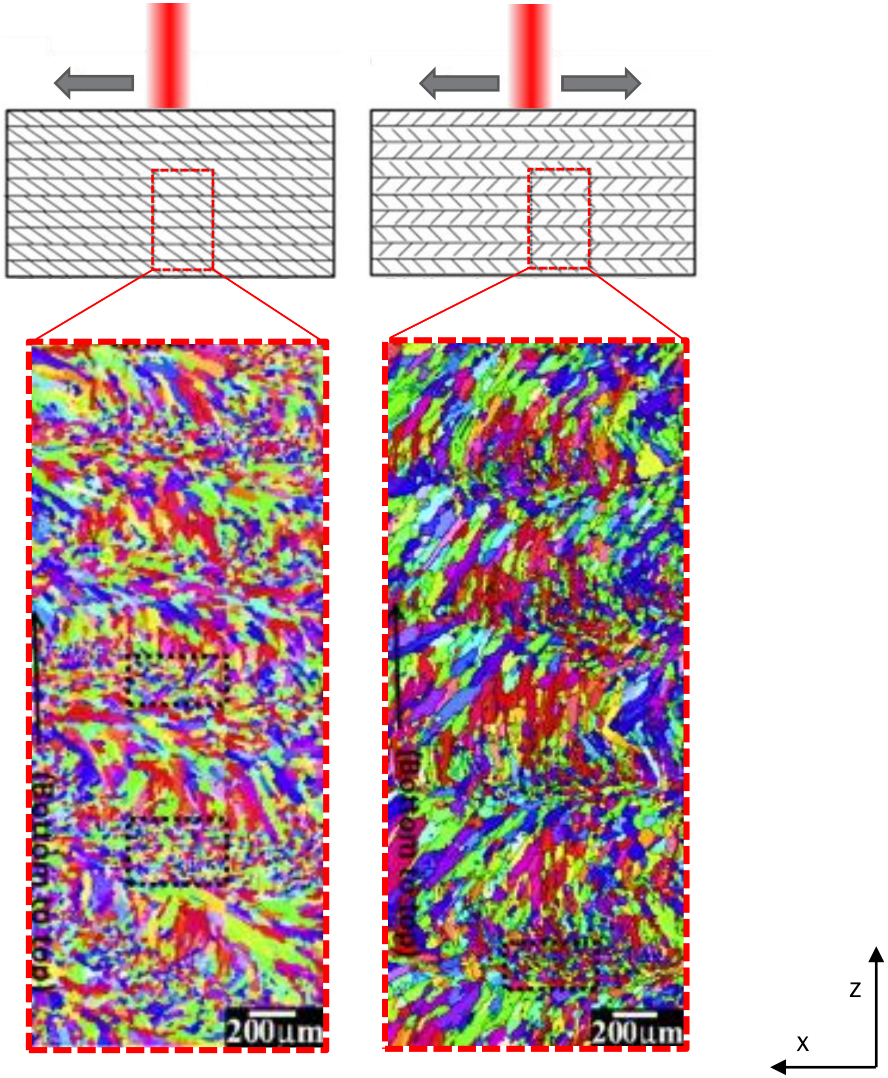

Parimi, Lakshmi L., et al. "Microstructural and texture development in direct laser fabricated IN718." *Materials Characterization* 89 (2014): 102-111.
Dinda, G. P., A. K. Dasgupta, and J. Mazumder. "Texture control during laser deposition of nickel-based superalloy." *Scripta Materialia* 67.5 (2012): 503-506.

Effect of scanning strategy

Melt pool shape – transverse section

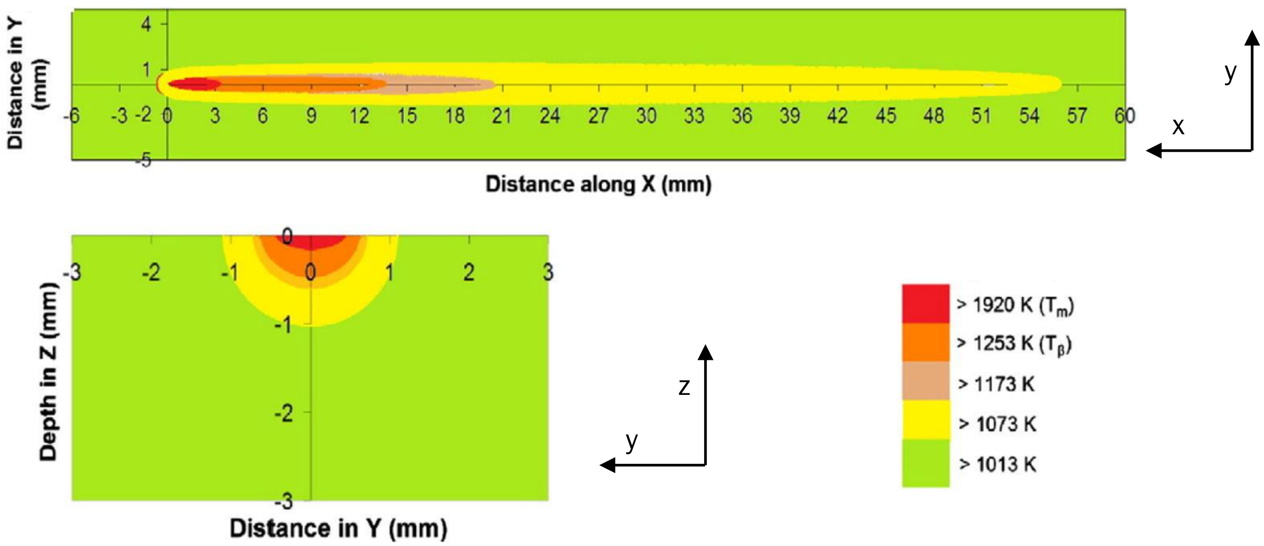

Although the melt pools is very elongated in the horizontal and longitudinal sections, the transverse section of the melt pool shows a hemispheric shape.

In the transverse cross-section, the directions of the columnar grains are perpendicular to the melt pool boundary.

DebRoy, Tarasankar, et al. "Additive manufacturing of metallic components–process, structure and properties." *Progress in Materials Science* 92 (2018): 112-224.

Microstructure control through processing

- Introduction: effect of thermal history on microstructure genesis
- Effect of scanning strategy
    - Effect of scanning direction
    - Effect of scanning length
- Effect of process parameters
- Effect of build geometry
- Effect of beamshaping
- Hybrid manufacturing
    - WAAM + rolling
    - LPBF + LSP

Effect of scanning length

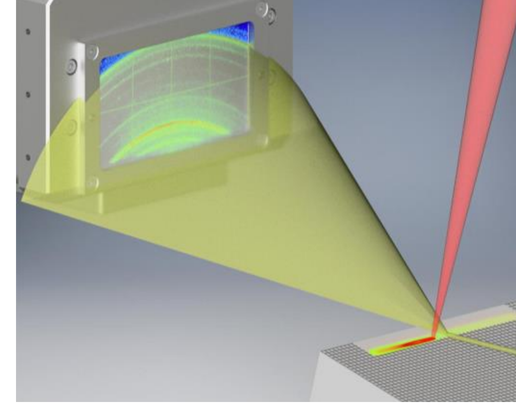

Operando X-ray diffraction: allows to follow the phase evolution during printing, shown as an intensity vs. diffraction angle and time by stacking thousands of individual diffraction patterns.

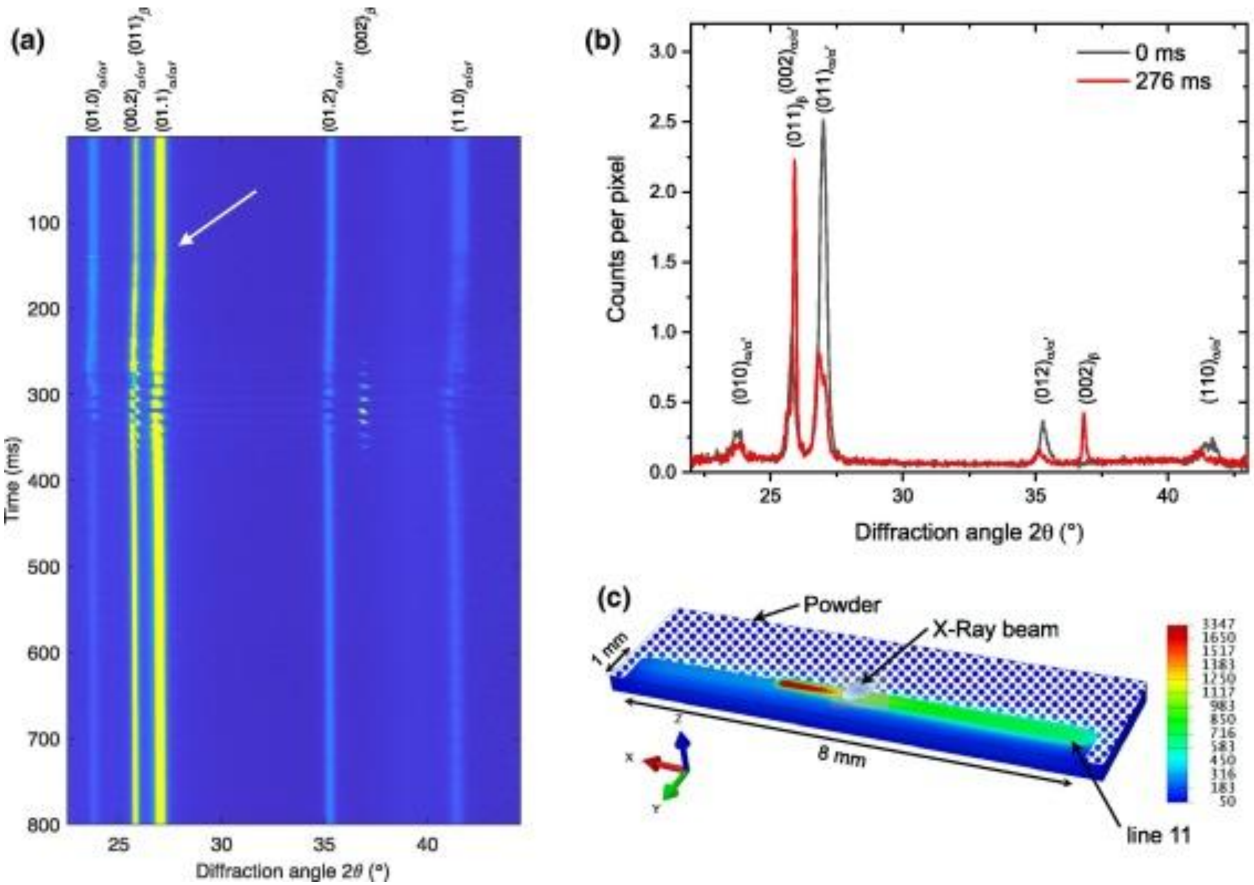

Hocine, Samy, et al. "Operando X-ray diffraction during laser 3D printing." *Materials Today* 34 (2020): 30-40.

Effect of scanning length

Operando X-ray diffraction: allows to follow the phase evolution during printing, shown as an intensity vs. diffraction angle and time by stacking 16 000 individual diffraction patterns.

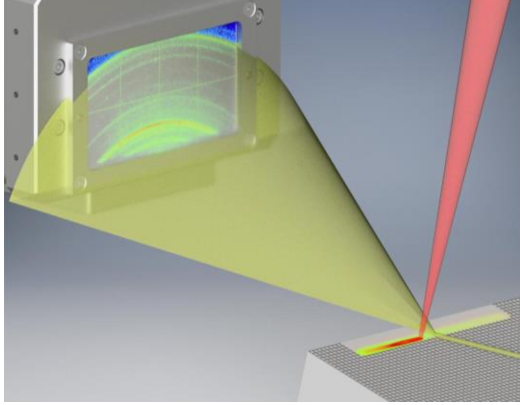

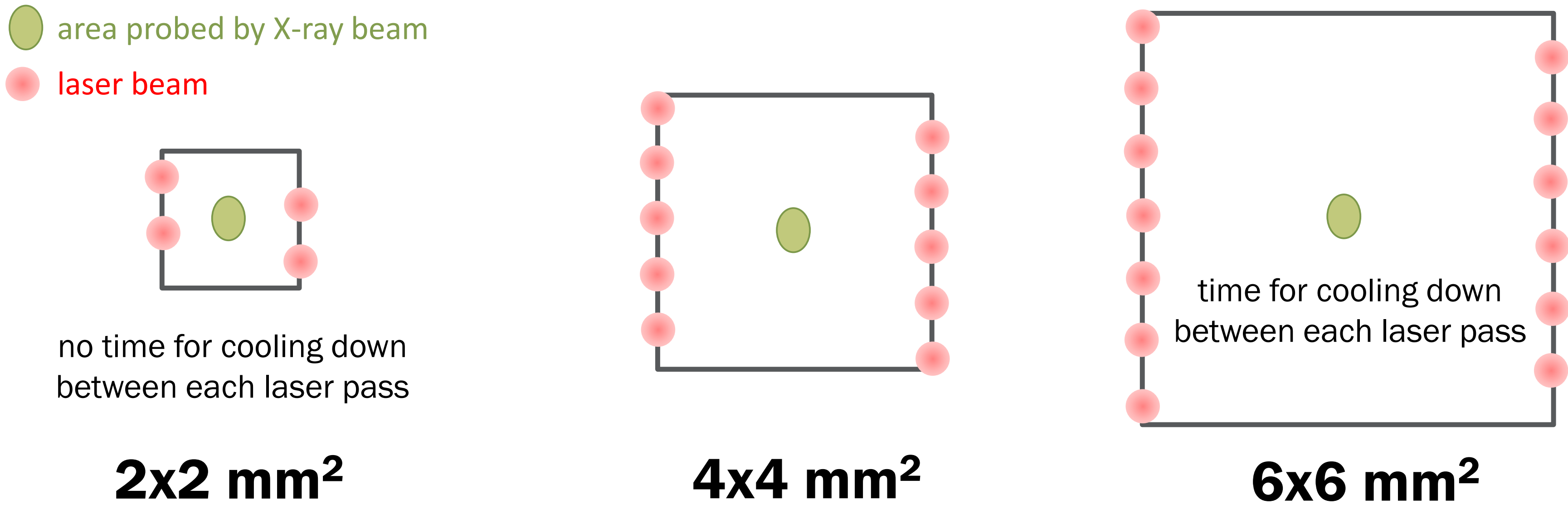

Increasing the length of the scanning vector changes the thermal history of the material. The area probed by the X-ray beam remains in the β phase during **70 ms (17 cycles) in the 2x2 mm²** square and **45 ms (7 cycles) in the 4×4 mm²** square. For the 6x6 mm² square, in each cycle β is transformed back to the α phase during cool down.

Hocine, Samy, et al. "Operando X-ray diffraction during laser 3D printing." *Materials Today* 34 (2020): 30-40.

Effect of scanning length

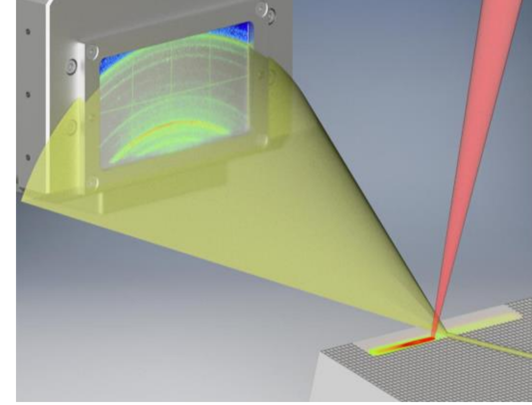

Operando X-ray diffraction: allows to follow the phase evolution during printing, shown as an intensity vs. diffraction angle and time by stacking 16 000 individual diffraction patterns.

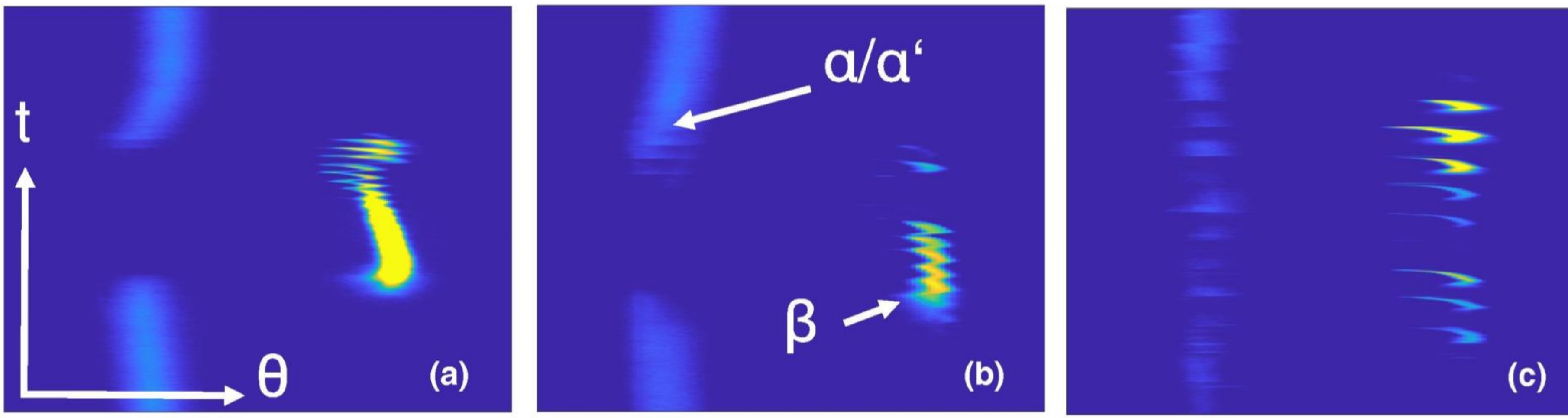

2x2 mm² **4x4 mm²** **6x6 mm²**

By increasing the length of the scanning vector the high temperature β-phase exists over a shorter time and exhibits higher cooling rates.

Hocine, Samy, et al. "Operando X-ray diffraction during laser 3D printing." *Materials Today* 34 (2020): 30-40.

Effect of scanning length

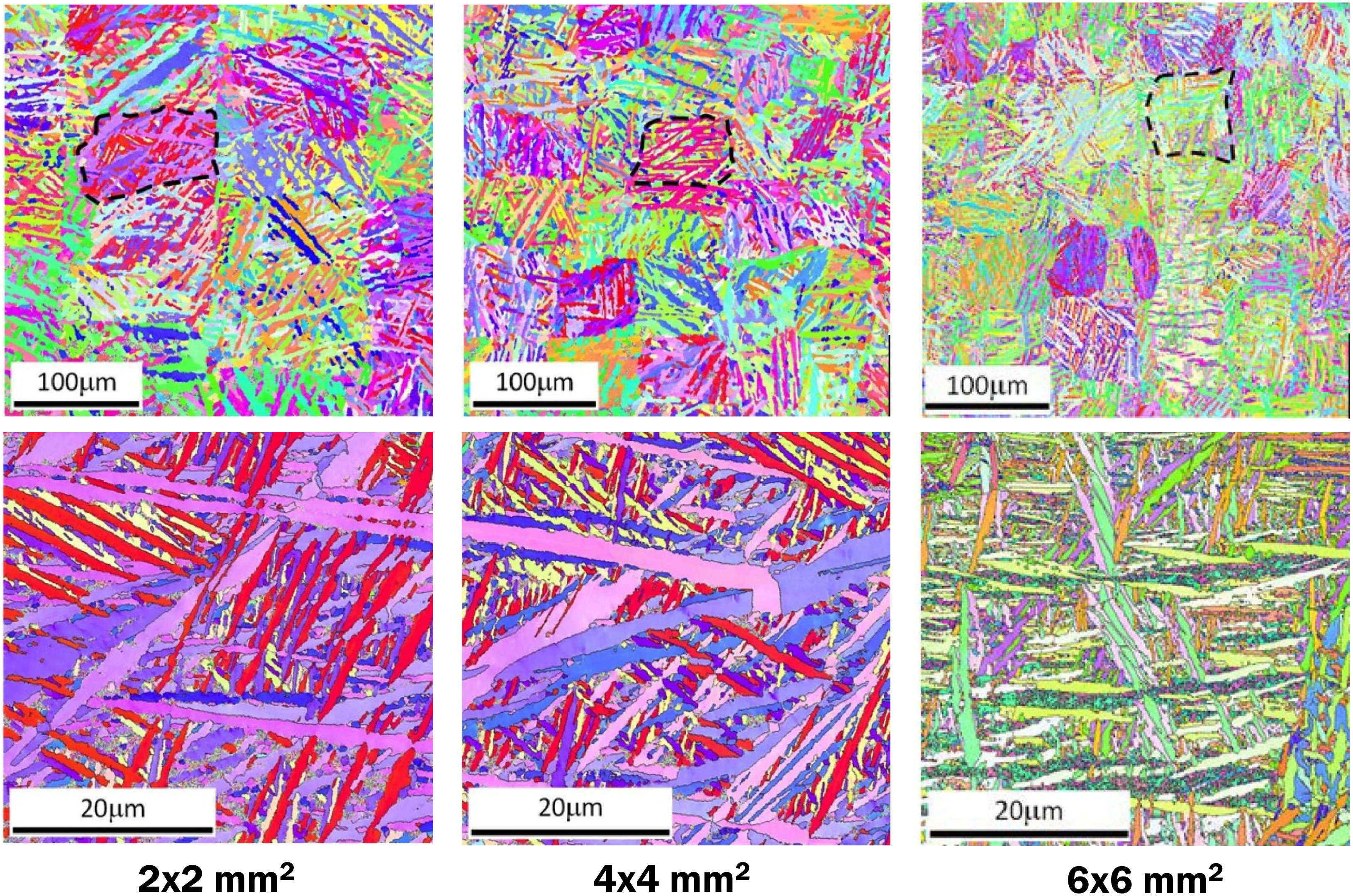

Hocine, Samy, et al. "Operando X-ray diffraction during laser 3D printing." *Materials Today* 34 (2020): 30-40.

Ti64 – LPBF

Effect of scanning length

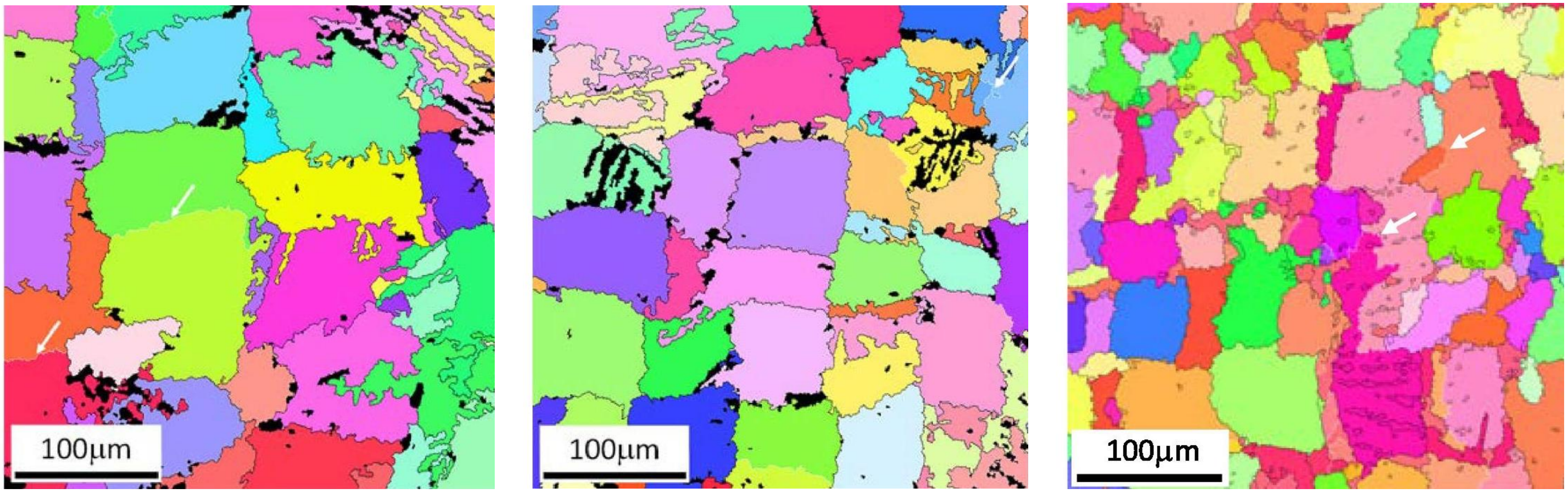

2x2 mm² **4x4 mm²** **6x6 mm²**

Numerical reconstruction of the parent β grains.

β grains are larger in the 2x2 mm^2 than in the 6x6 mm^2
due to the material staying above the β transus for a longer time

Hocine, Samy, et al. "Operando X-ray diffraction during laser 3D printing." *Materials Today* 34 (2020): 30-40.

Microstructure control through processing

- Introduction: effect of thermal history on microstructure genesis
- Effect of scanning strategy
  - Effect of scanning direction
  - Effect of scanning length
- Effect of process parameters
- Effect of build geometry
- Effect of beamshaping
- Hybrid manufacturing
  - WAAM + rolling
  - LPBF + LSP

Effect of process parameters: scanning speed

Effect of scanning speed on melt pool geometry

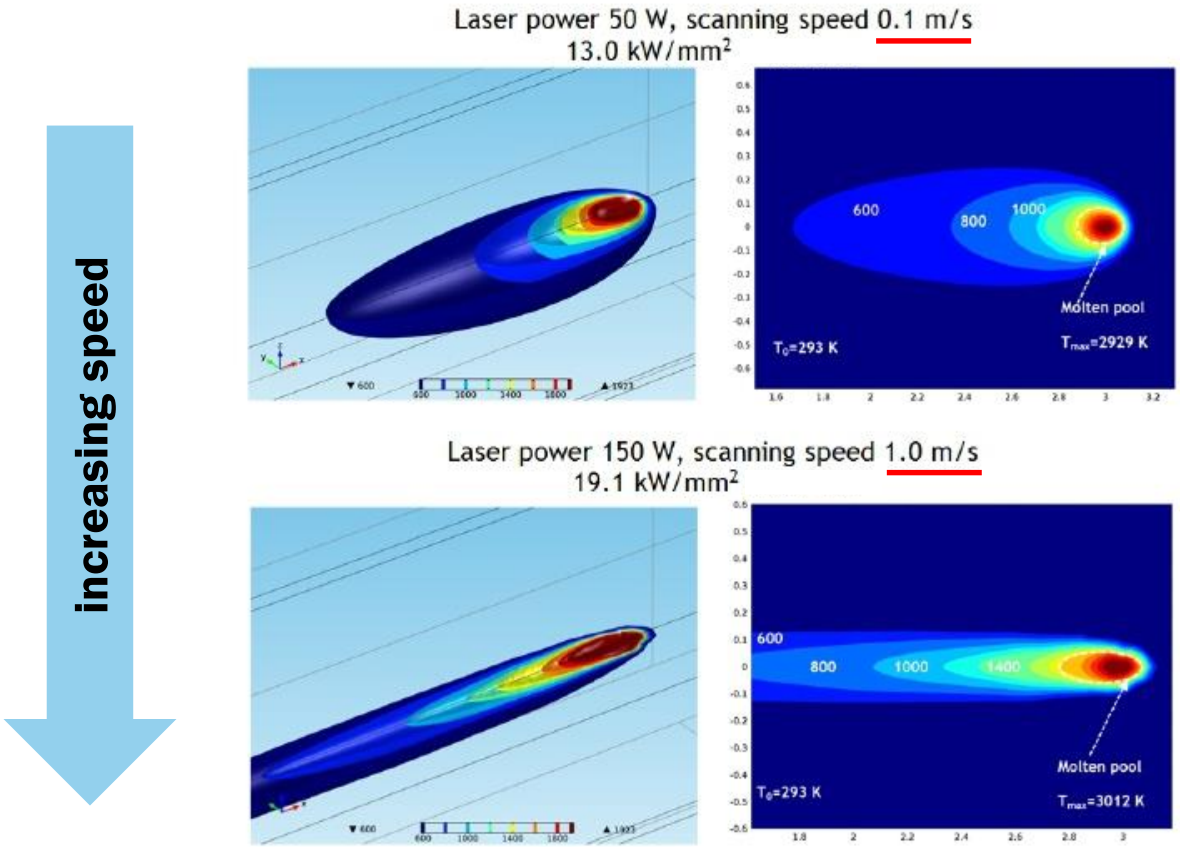

By increasing the scanning speed, the melt pool tends to become more elongated, hence favoring a vertical orientation of the grains.

Yadroitsava, Ina, et al. "Peculiarities of single track formation from Ti6AL4V alloy at different laser power densities by selective laser melting." *South African Journal of Industrial Engineering* 26.3 (2015): 86-95.

Effect of process parameters: scanning speed

Effect of scanning speed on grain size

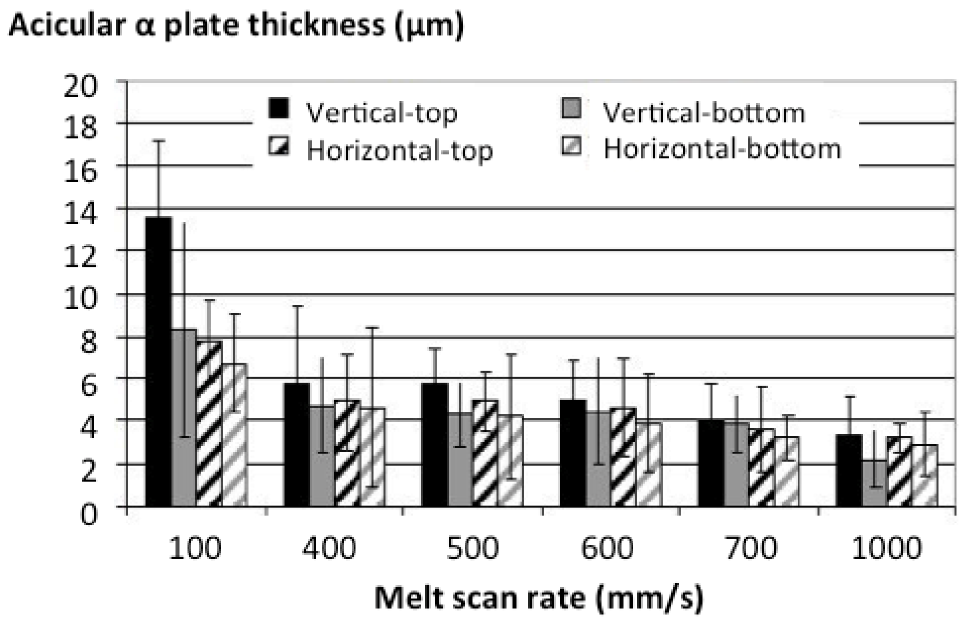

higher scan speed ⟶ faster cooling ⟶ smaller grain size

IN718 – DED

Effect of process parameters: power

Effect of power on cellular spacing

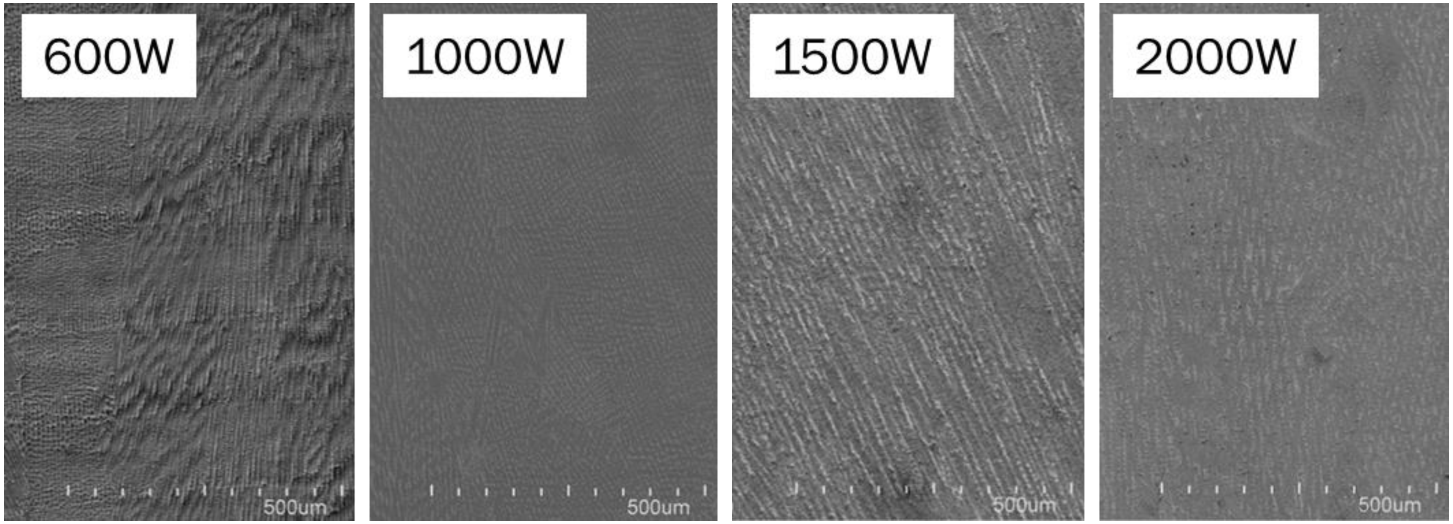

The dendrite arm spacing increases with increasing power
(lower cooling rate)

Effect of process parameters: preheating

Effect of preheating on grain shape

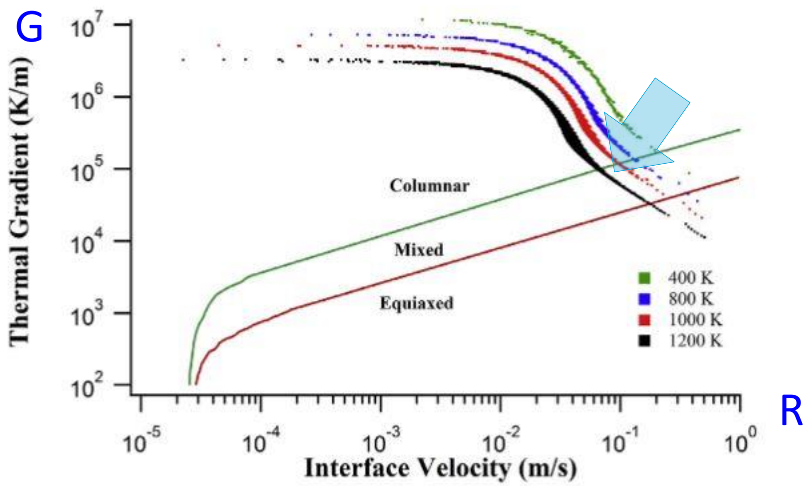

Change in temperature gradient G and liquid-solid interface velocity R of spot melt as a function of preheat temperature.

The volume fraction of equiaxed grains increases with an increase in preheat temperature.

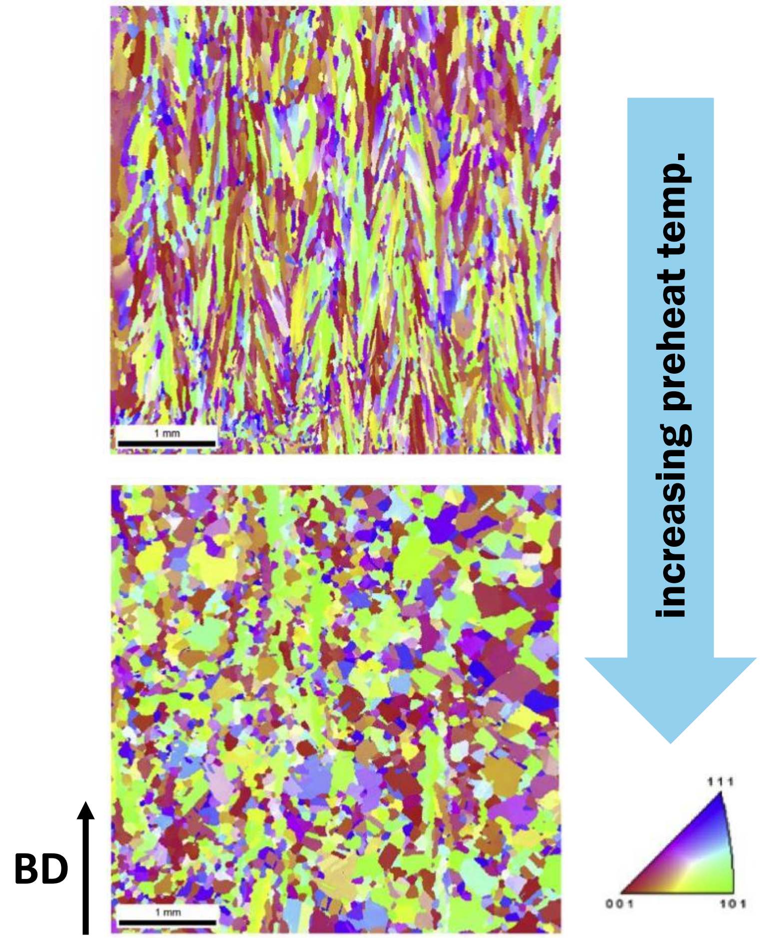

Raghavan, Narendran, et al. "Numerical modeling of heat-transfer and the influence of process parameters on tailoring the grain morphology of IN718 in electron beam additive manufacturing." *Acta Materialia* 112 (2016): 303-314.

Effect of process parameters: preheating

Effect of preheating on grain size

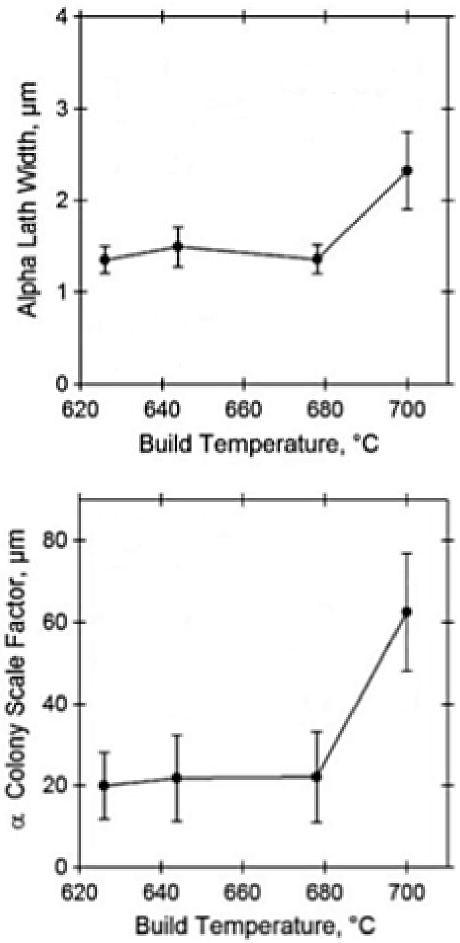

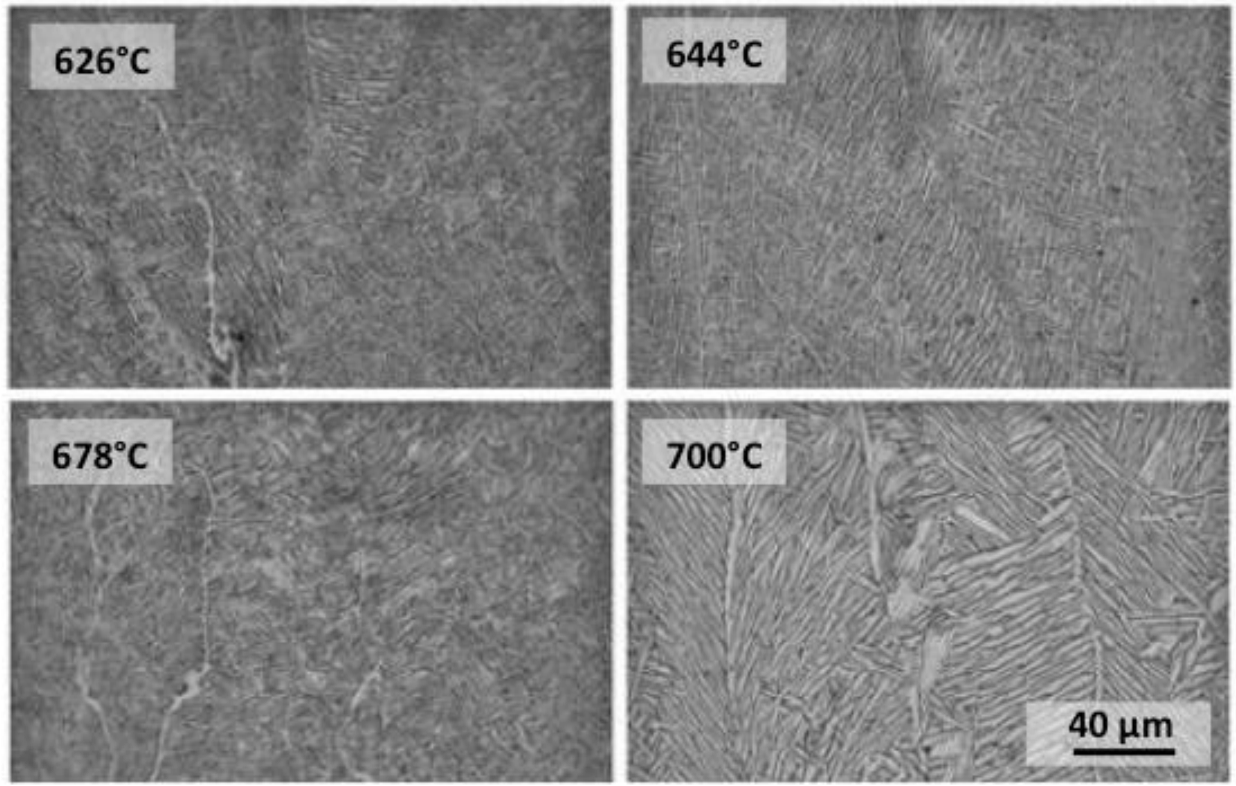

Al-Bermani, S. S., et al. "The origin of microstructural diversity, texture, and mechanical properties in electron beam melted Ti-6Al-4V." *Metallurgical and materials transactions a* 41.13 (2010): 3422-3434.

Effect of process parameters: layer thickness

30 µm layer thickness:
acicular α′ martensite

60 µm and 90 µm layer thickness:
ultrafine lamellar (α + β) structure.

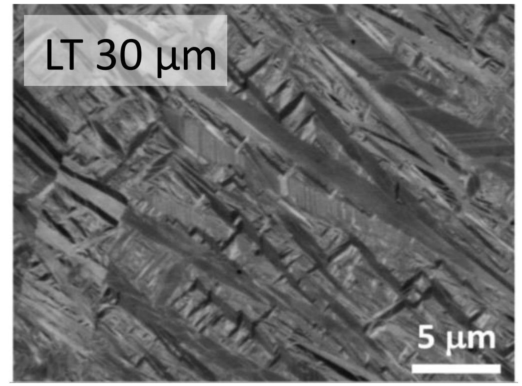

P = 175W
v = 710 mm/s

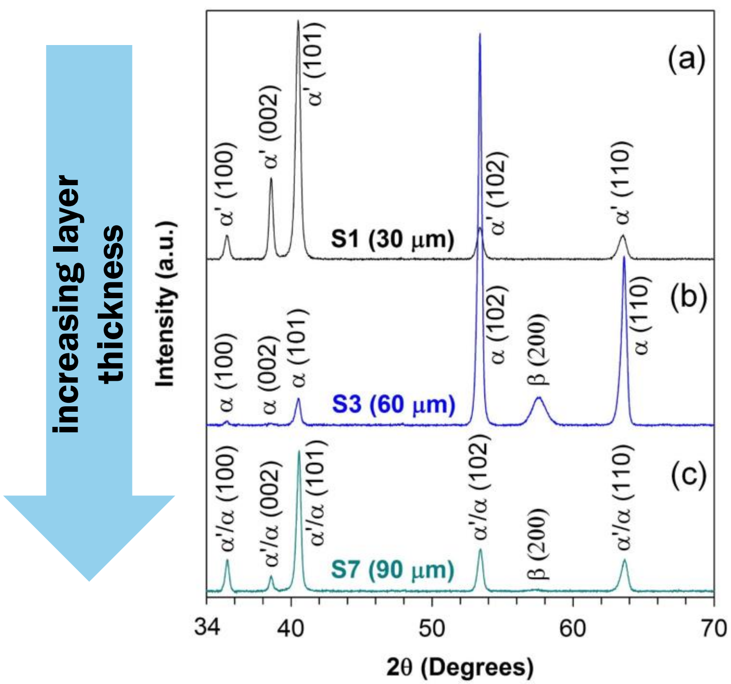

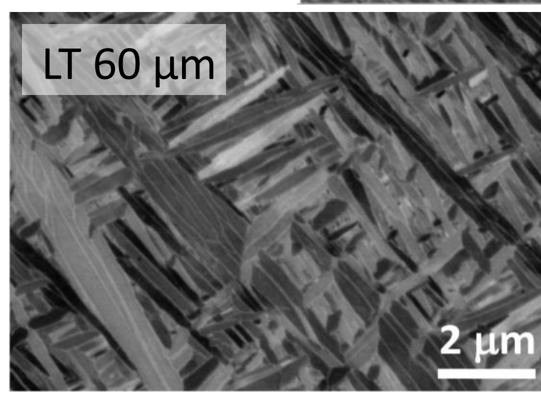

P = 375W
v = 1029 mm/s

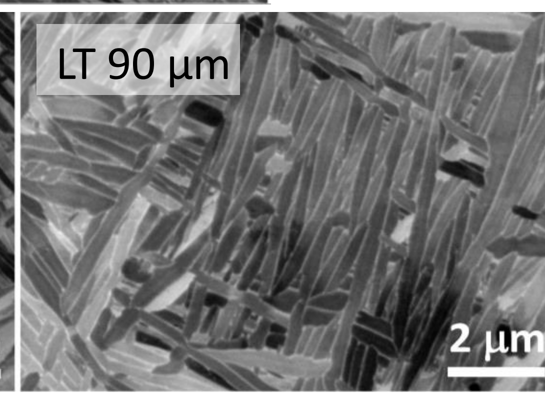

P = 375W
v = 686 mm/s

increase in layer thickness (larger melt pool)
⇒ lower cooling rate, possible martensite decomposition

Xu, Wei, et al. "Additive manufacturing of strong and ductile Ti–6Al–4V by selective laser melting via in situ martensite decomposition." *Acta Materialia* 85 (2015): 74-84.

Ti64 – LPBF

Effect of process parameters: inter-layer time

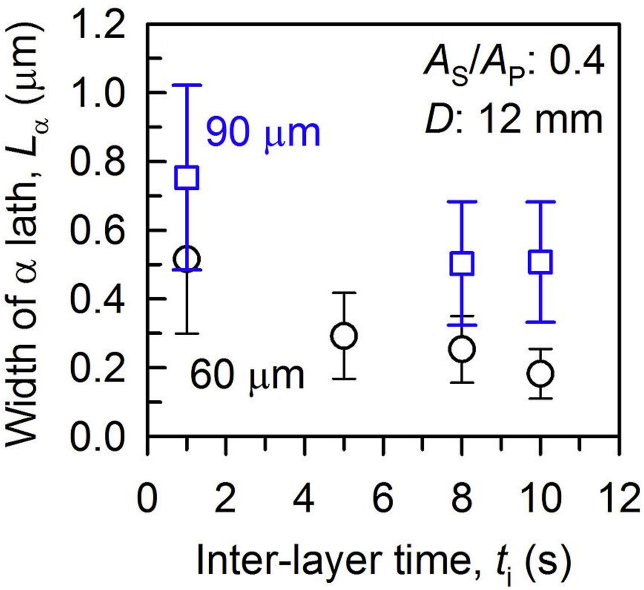

A longer inter-layer time is not beneficial to achieve the lamellar (α+β) microstructure: with an increase in t_i from 1s to 10s, the width of α laths substantially decreases.

The inter-layer time is a decisive factor in promoting in-situ martensite decomposition for the achievement of a lamellar (α+β) microstructure.

increasing inter-layer time

- Lower average temperature
- Higher cooling rate
- Finer microstructure / favours martensite

Xu, Wei, et al. "In situ tailoring microstructure in additively manufactured Ti-6Al-4V for superior mechanical performance." *Acta Materialia* 125 (2017): 390-400.

Ti64 – LPBF

Effect of process parameters: supports

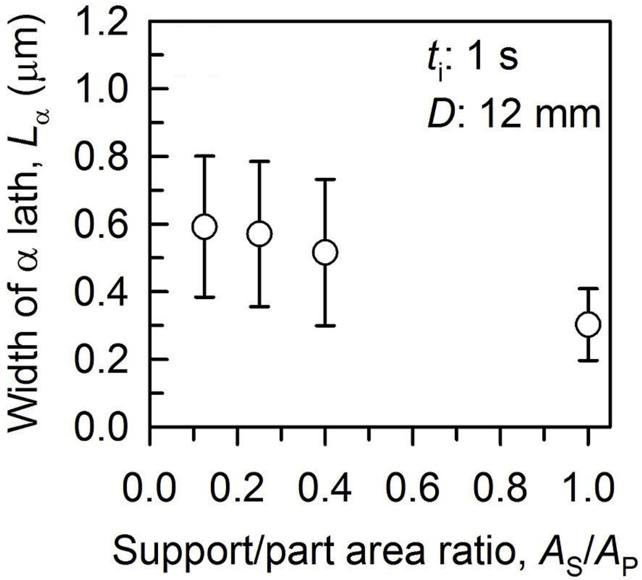

increasing contact area between supports and part

The increase in contact area leads to finer lamellar microstructure, due to higher cooling rates.

Combined with the tuning of other process parameters, the use of smaller support/part contact area can favor more significant in-situ martensite decomposition.

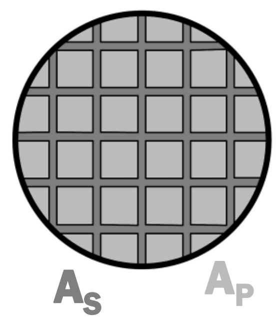

Xu, Wei, et al. "In situ tailoring microstructure in additively manufactured Ti-6Al-4V for superior mechanical performance." *Acta Materialia* 125 (2017): 390-400.

TC11 – DED

Effect of process parameters: mass deposition rate (DED)

Effect of mass deposition rate on grain shape

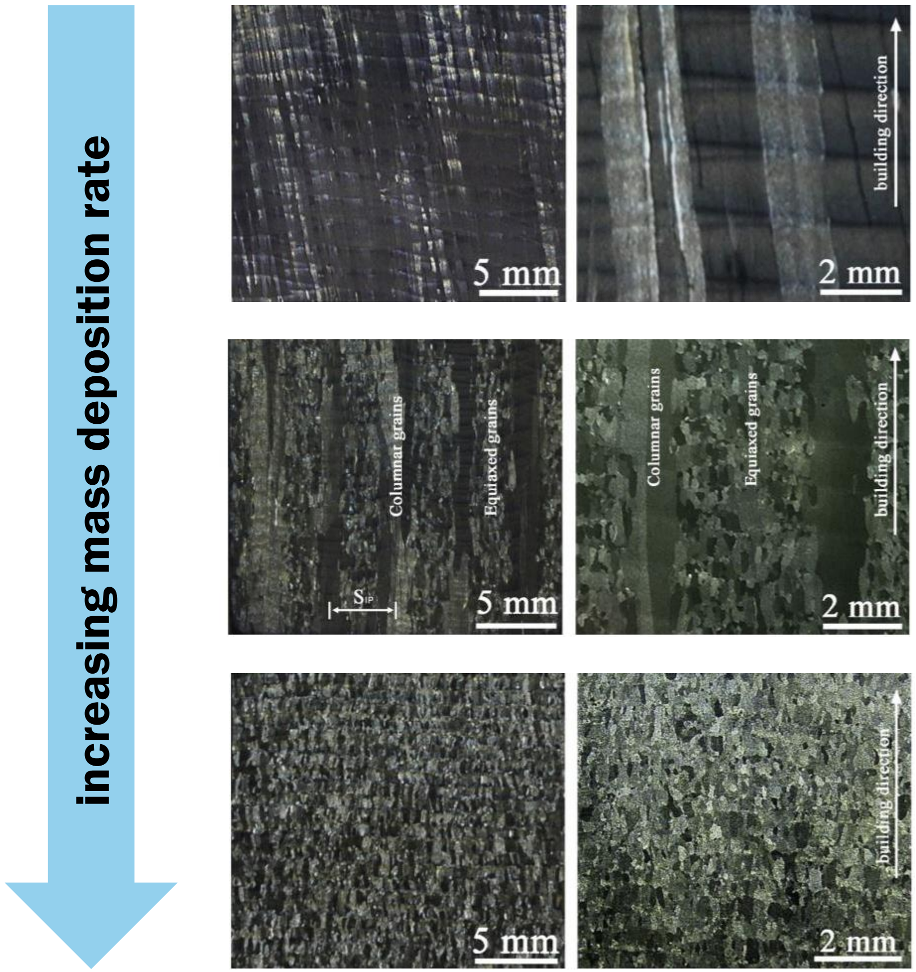

Mass deposition rate: 10 g/min

Mass deposition rate: 25 g/min

Mass deposition rate: 50 g/min

Wang, T., et al. "Grain morphology evolution behavior of titanium alloy components during laser melting deposition additive manufacturing." *Journal of Alloys and Compounds* 632 (2015): 505-513.

Effect of process parameters: mass deposition rate (DED)

Effect of mass deposition rate on grain shape

Grain structures in a single line scan:

Large columnar grains in the near pool-bottom region: product of direct epitaxial grain growth from the parent grains at the pool bottom.

Fine equiaxed grains in the near surface region: newly nucleated at the pool surface and within the pool on partially melted powders as heterogeneous nucleation sites.

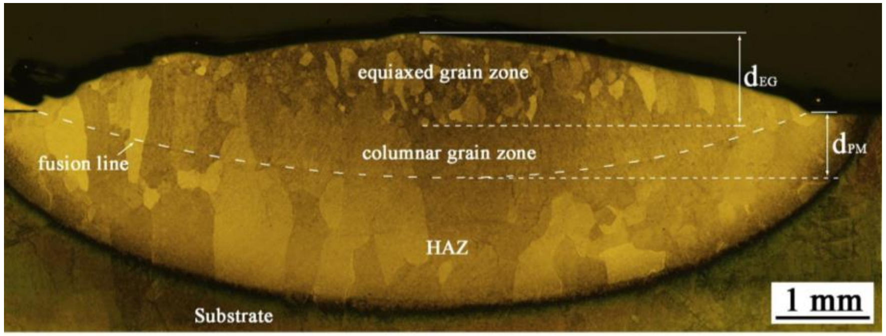

The fraction of equiaxed grains increases substantially with the increasing mass deposition rate.

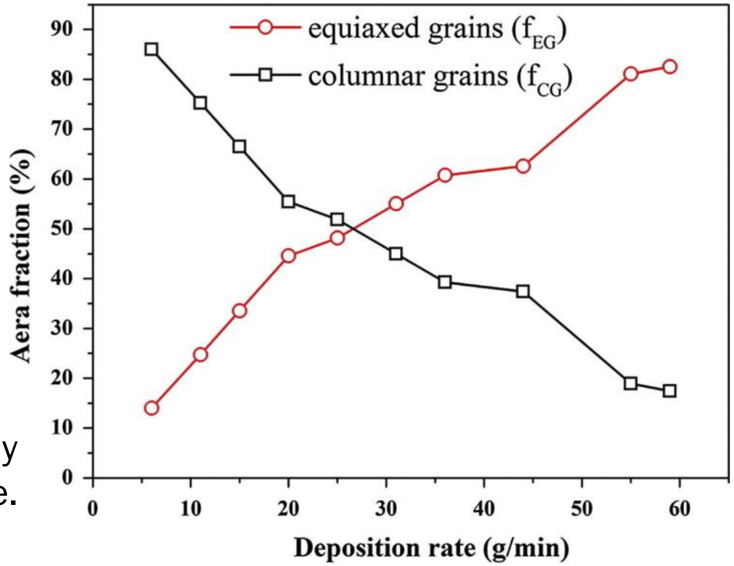

Wang, T., et al. "Grain morphology evolution behavior of titanium alloy components during laser melting deposition additive manufacturing." *Journal of Alloys and Compounds* 632 (2015): 505-513.

Effect of process parameters: mass deposition rate (DED)

Effect of mass deposition rate on grain shape

Grain structures in <u>a single line scan</u>:

Two competing mechanisms:

- heterogeneous nucleation on the pool surface and in the melt pool on the partially melted powder particles
- epitaxial growth from the parent grains at the pool bottom

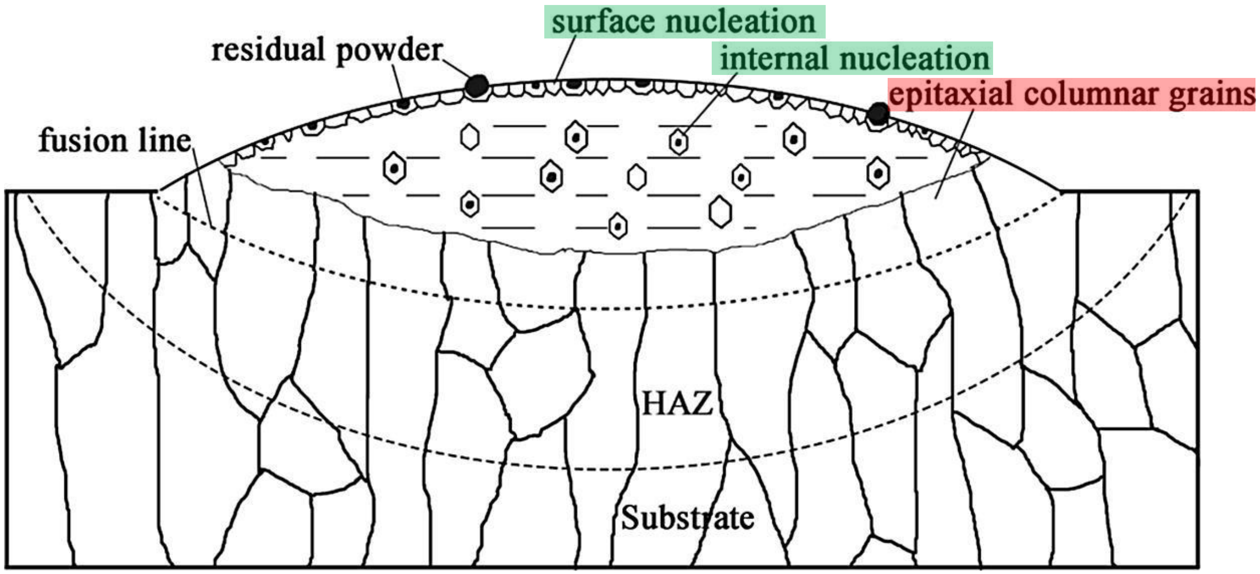

Wang, T., et al. "Grain morphology evolution behavior of titanium alloy components during laser melting deposition additive manufacturing." *Journal of Alloys and Compounds* 632 (2015): 505-513.

TC11 – DED

Effect of process parameters: mass deposition rate (DED)

Effect of mass deposition rate on grain shape

Grain structures in a single line scan:

Two competing mechanisms:

- heterogeneous nucleation on the pool surface and in the melt pool on the partially melted powder particles
- epitaxial growth from the parent grains at the pool bottom

Lower mass deposition rate:

⇒ higher excessive energy input for a more complete melting of the powder

1. less residual powder particles at the pool surface and within the melt pool

   ⇒ less heterogeneous nucleation sites

   ⇒ lower fraction of equiaxed grains

2. larger penetration re-melting depth

   ⇒ more favorable epitaxial growth from the parent grains at the pool bottom

Wang, T., et al. "Grain morphology evolution behavior of titanium alloy components during laser melting deposition additive manufacturing." *Journal of Alloys and Compounds* 632 (2015): 505-513.

Microstructure control through processing

- Introduction: effect of thermal history on microstructure genesis
- Effect of scanning strategy
  - Effect of scanning direction
  - Effect of scanning length
- Effect of process parameters
- Effect of build geometry
- Effect of beamshaping
- Hybrid manufacturing
  - WAAM + rolling
  - LPBF + LSP

Effect of build geometry

Effect of build geometry on grain shape

increasing wall thickness

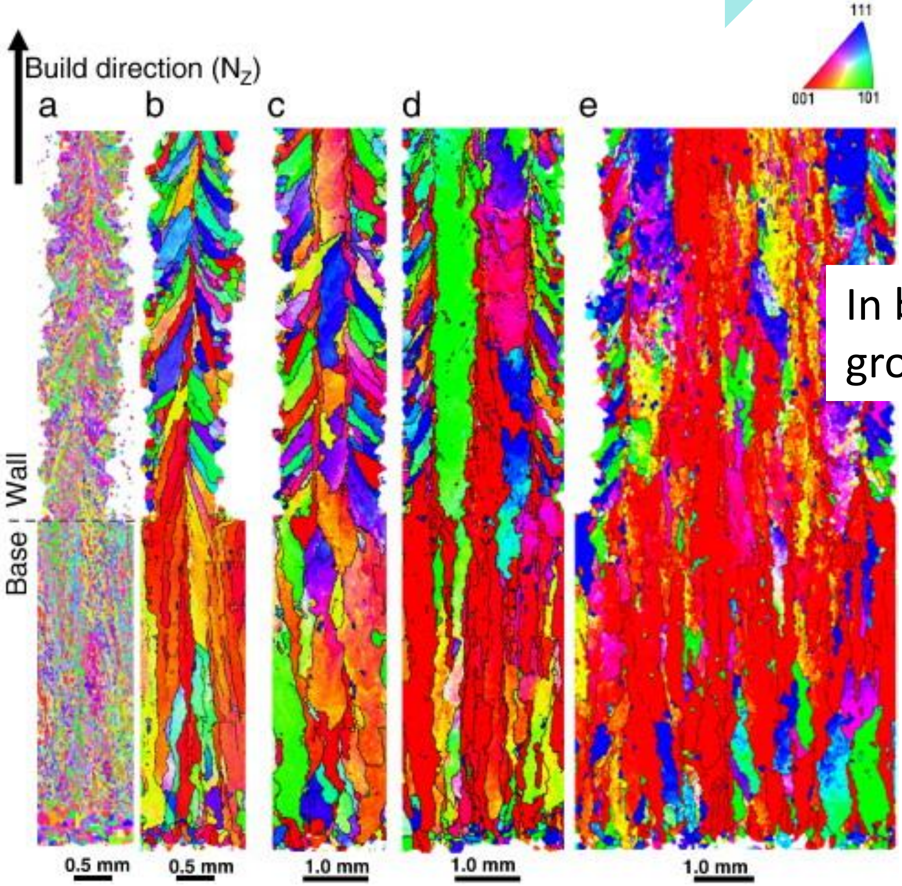

In bulk sections: coarse columnar grains grow normal to the deposited layers

Antonysamy, A.A., J. Meyer, and P. B. Prangnell. "Effect of build geometry on the β-grain structure and texture in additive manufacture of Ti6Al4V by selective electron beam melting." Materials characterization 84 (2013): 153-168.

Effect of build geometry

Effect of build geometry on grain shape

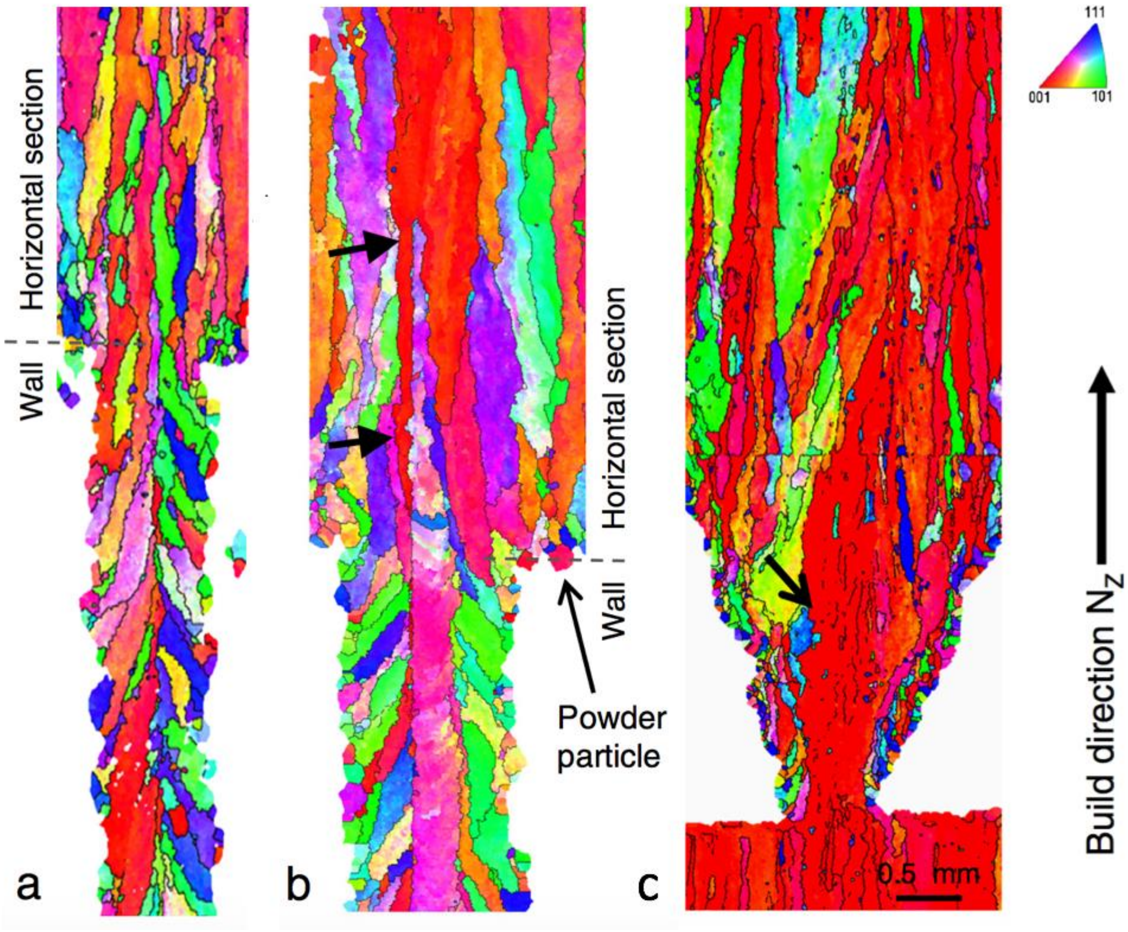

Antonysamy, A.A., J. Meyer, and P. B. Prangnell. "Effect of build geometry on the β-grain structure and texture in additive manufacture of Ti6Al4V by selective electron beam melting." Materials characterization 84 (2013): 153-168.

Effect of build geometry

Effect of build geometry on grain size

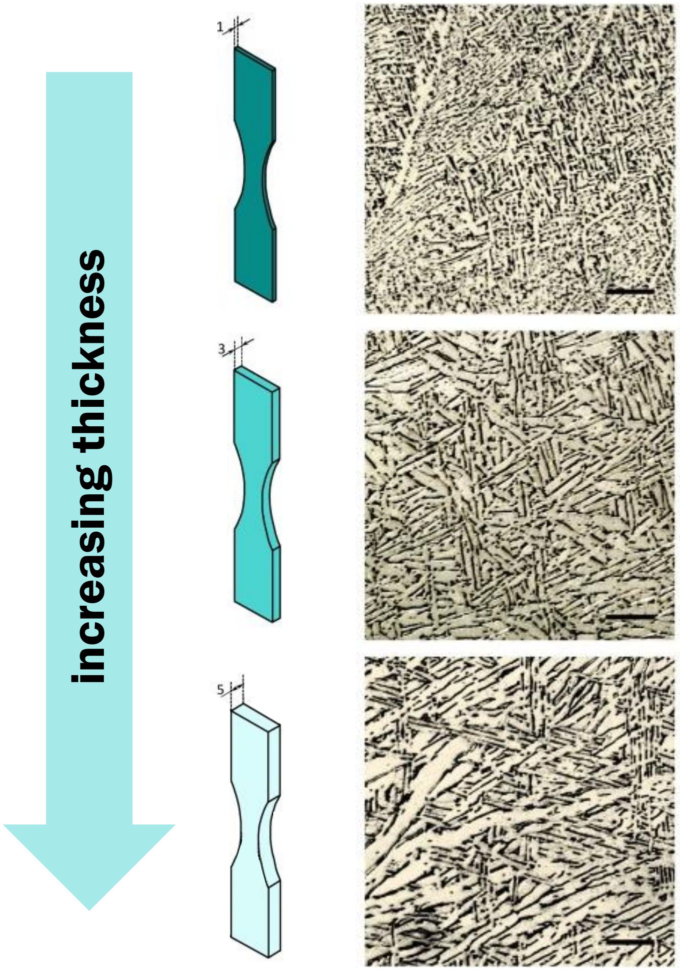

α plate thickness

0.7 µm

1.3 µm

1.9 µm

lower cooling rate in thicker specimens
⇒ larger grain size

Razavi, S. M. J., B. Van Hooreweder, and F. Berto. "Effect of build thickness and geometry on quasi-static and fatigue behavior of Ti-6Al-4V produced by Electron Beam Melting." *Additive Manufacturing* 36 (2020): 101426.

Ti64 – EBM

Effect of distance from the build plate

Effect of distance from the build plate on grain size

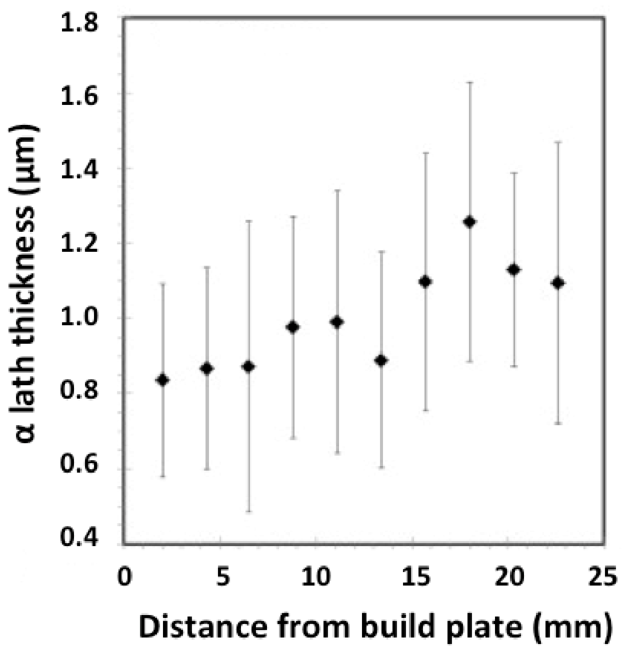

Increasing α lath thickness with increasing distance from the build plate

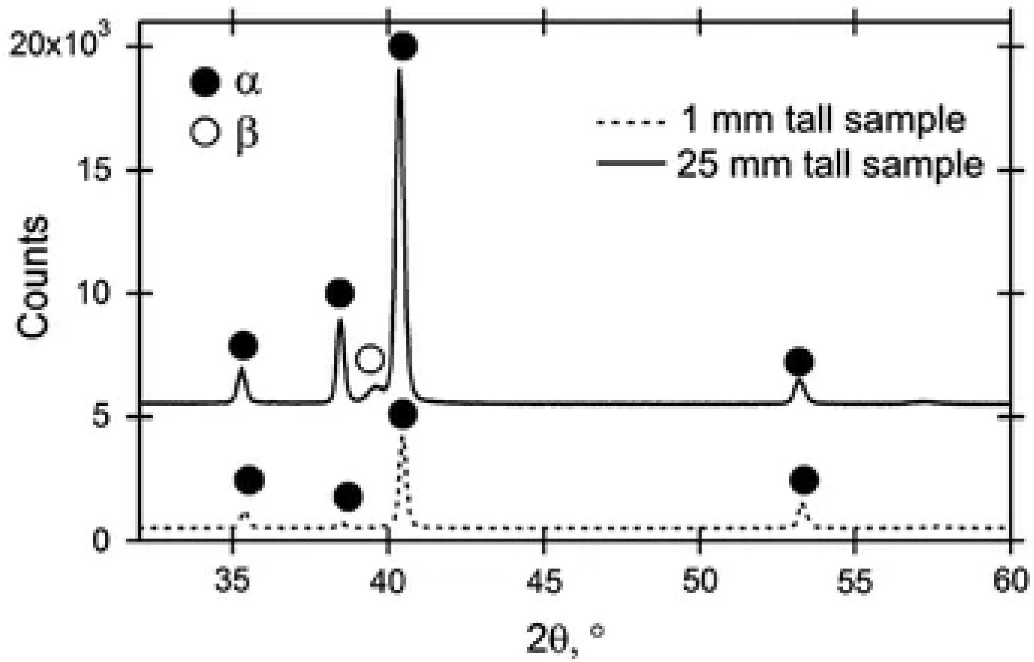

Evidence of α' martensite in small (1mm tall) samples and α+β in long (25mm) samples

Al-Bermani, S. S., et al. "The origin of microstructural diversity, texture, and mechanical properties in electron beam melted Ti-6Al-4V." *Metallurgical and materials transactions a* 41.13 (2010): 3422-3434.

Microstructure control through processing

- Introduction: effect of thermal history on microstructure genesis
- Effect of scanning strategy
  - Effect of scanning direction
  - Effect of scanning length
- Effect of process parameters
- Effect of build geometry
- Effect of beamshaping
- Hybrid manufacturing
  - WAAM + rolling
  - LPBF + LSP

Effect of beam shaping

Beam shaping = introduction of an added degree of freedom in process optimization

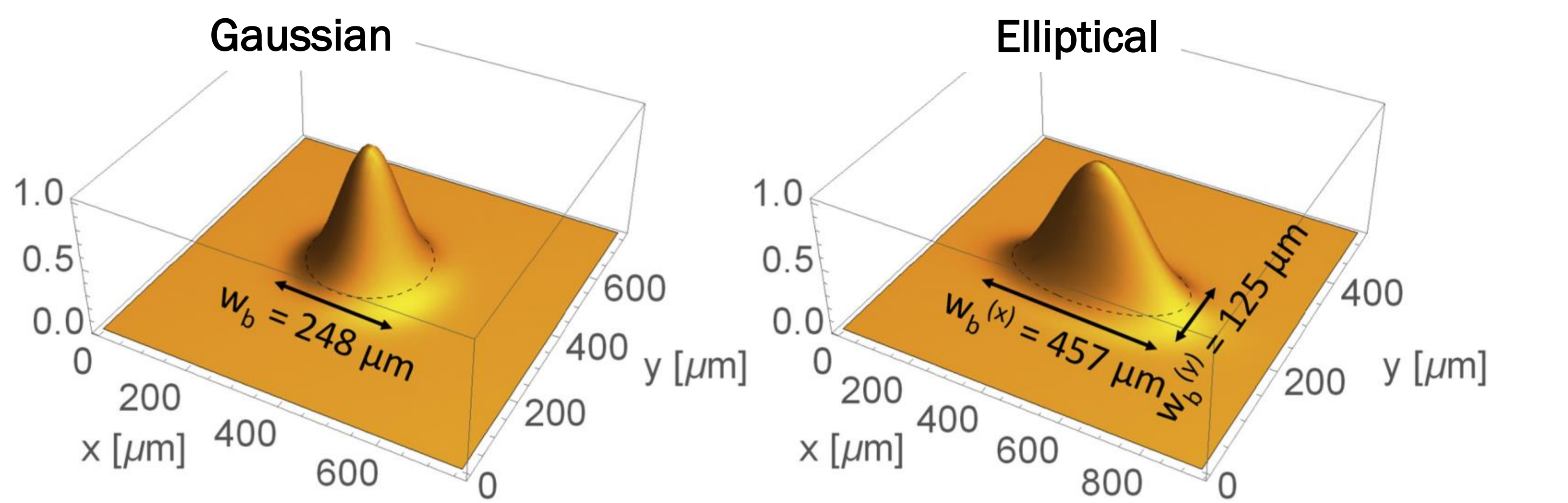

Gaussian laser intensity profiles are standard in laser-based metal additive manufacturing.

Using an optical set-up, the beam ellipticity and size can be adjusted.

Beam shaping can modify the laser energy distribution and temperature gradient on the melt pool surface, hence affecting:

- the size of the overheated area
- Marangoni convection, recoil pressure and the corresponding stirring effect

Roehling, Tien T., et al. "Modulating laser intensity profile ellipticity for microstructural control during metal additive manufacturing." *Acta Materialia* 128 (2017): 197-206.

Effect of beam shaping

Gaussian

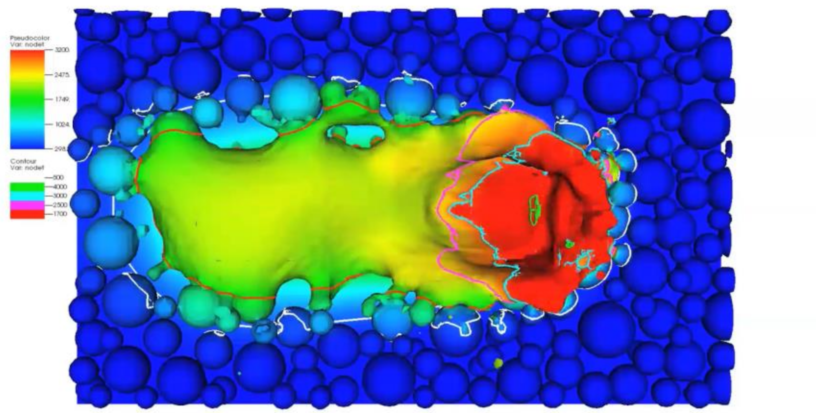

Elliptical - transverse

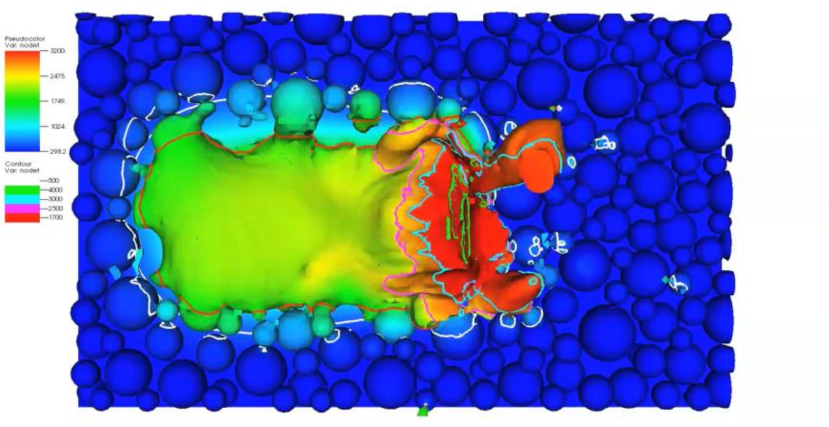

Elliptical - longitudinal

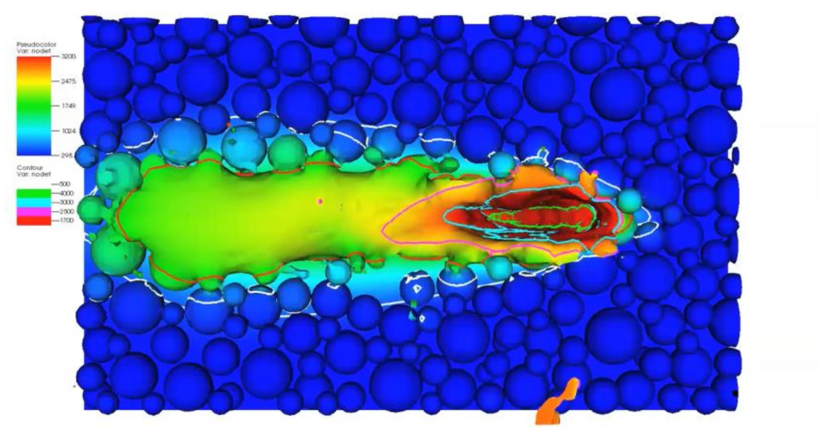

Roehling, Tien T., et al. "Modulating laser intensity profile ellipticity for microstructural control during metal additive manufacturing." *Acta Materialia* 128 (2017): 197-206.

316L – LPBF

Effect of beam shaping

Marangoni convection + recoil pressure effects

⇒ **melt vortex**, wherein hot molten metal is stirred from the depression towards the much cooler transition region at high velocity.

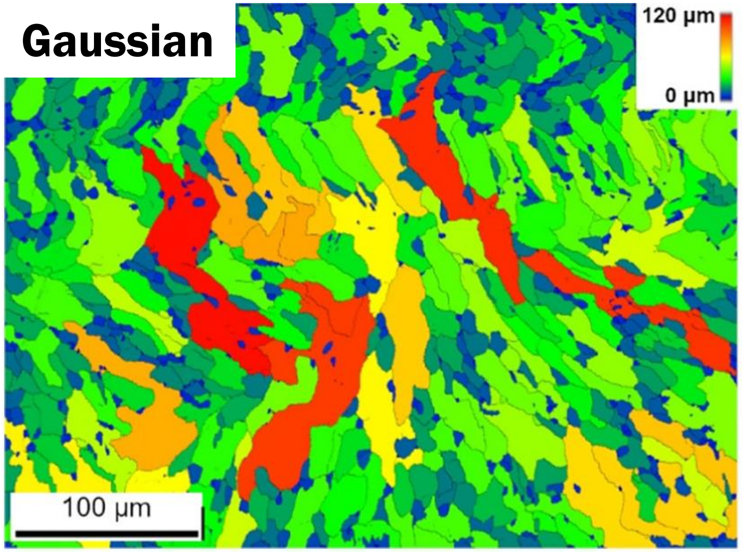

Elliptical intensity profile:

higher melt flow velocities than Gaussian profile.

⇒ dendrite tip fragmentation and redistribution

⇒ solid fragments acting as **nucleation sites** for equiaxed grains ahead of the growth front

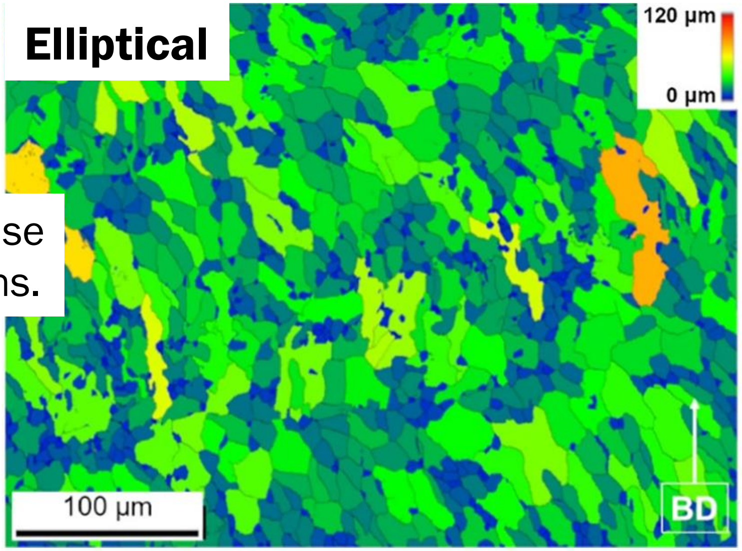

Using an elliptical beam can increase the volume fraction of equiaxed grains.

Roehling, Tien T., et al. "Controlling grain nucleation and morphology by laser beam shaping in metal additive manufacturing." *Materials & Design* 195 (2020): 109071.

Microstructure control through processing

- Introduction: effect of thermal history on microstructure genesis
- Effect of scanning strategy
  - Effect of scanning direction
  - Effect of scanning length
- Effect of process parameters
- Effect of build geometry
- Effect of beamshaping
- Hybrid manufacturing
  - WAAM + rolling
  - LPBF + LSP

Hybrid manufacturing: combining rolling and AM

Objective: refine the microstructure and transition from columnar to equiaxed morphology

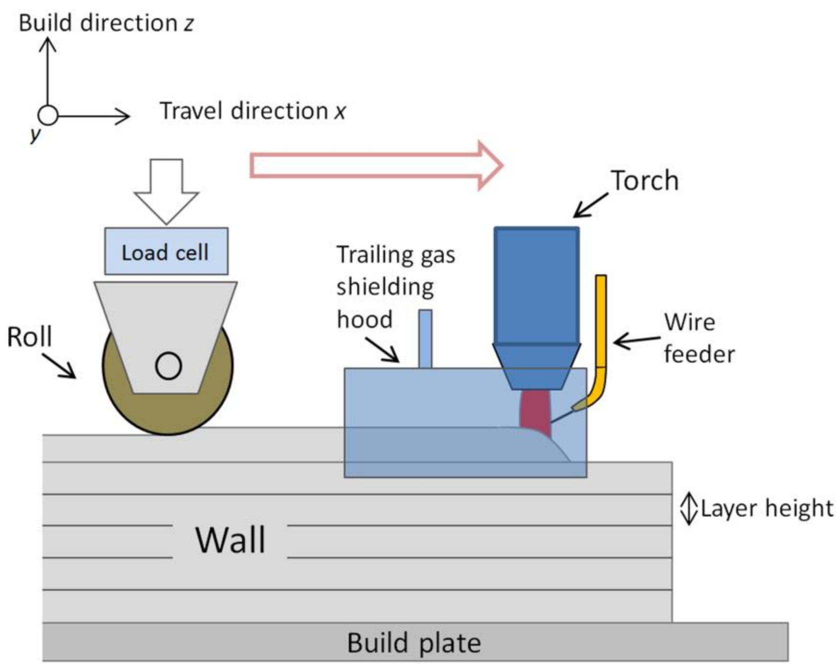

Wire–Arc Additive Manufacturing (WAAM)
A consumable wire is fed at a controlled rate into an electric arc (or plasma) welding torch that is translated by a robot.

A small deformation step is introduced with the deposition of each layer, using a roller integrated with the AM system.

The amount of plastic deformation introduced into each layer is sufficient for recrystallization of the β-grains to occur during re-heating, when the next layer is deposited.

Donoghue, J., et al. "The effectiveness of combining rolling deformation with Wire–Arc Additive Manufacture on β-grain refinement and texture modification in Ti–6Al–4V." *Materials Characterization* 114 (2016): 103-114.

Hybrid manufacturing: combining rolling and AM

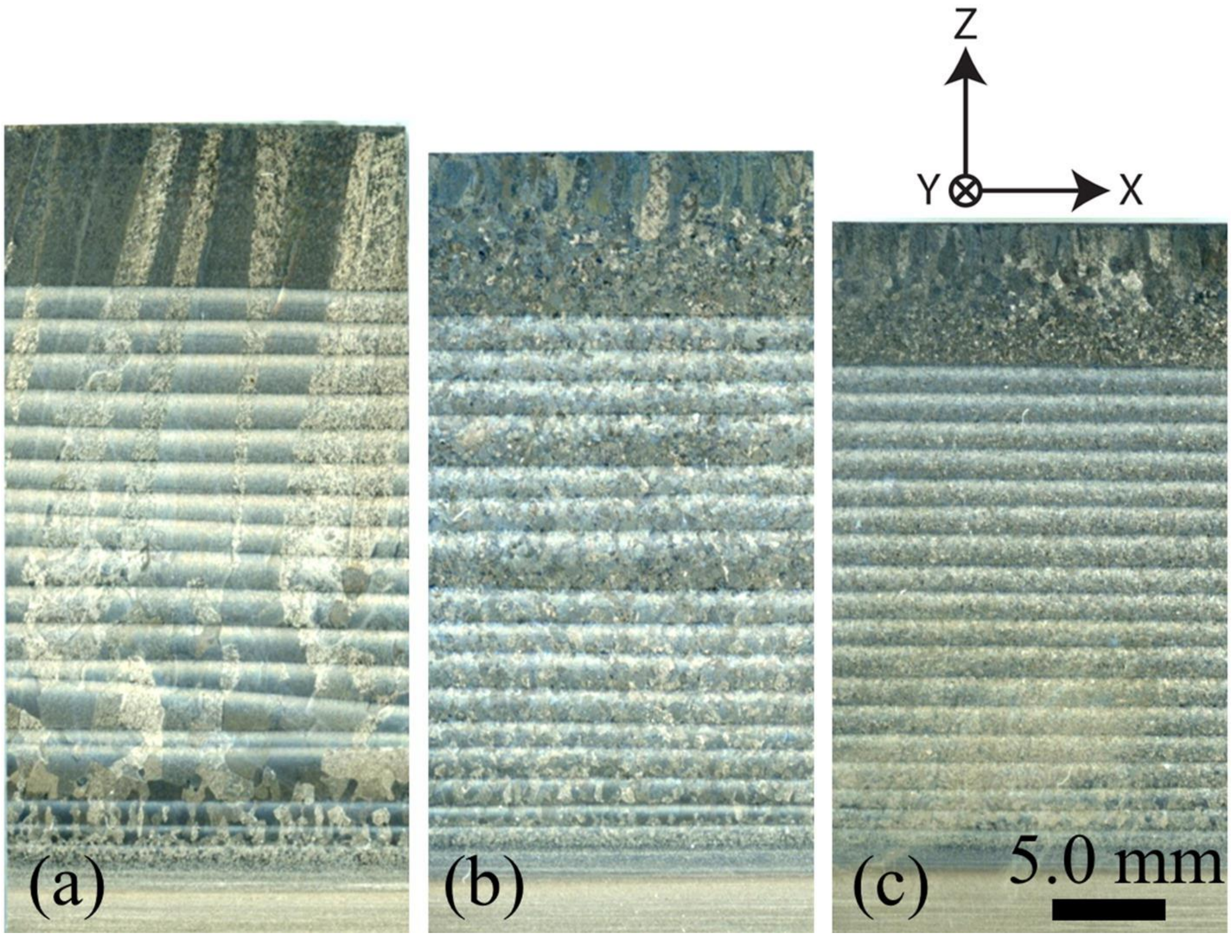

no rolling load | rolling load: 50kN | rolling load: 75kN

Donoghue, J., et al. "The effectiveness of combining rolling deformation with Wire–Arc Additive Manufacture on β-grain refinement and texture modification in Ti–6Al–4V." *Materials Characterization* 114 (2016): 103-114.

Ti64 – WAAM

Hybrid manufacturing: combining rolling and AM

Measured α-phase IPF orientation coloured EBSD maps

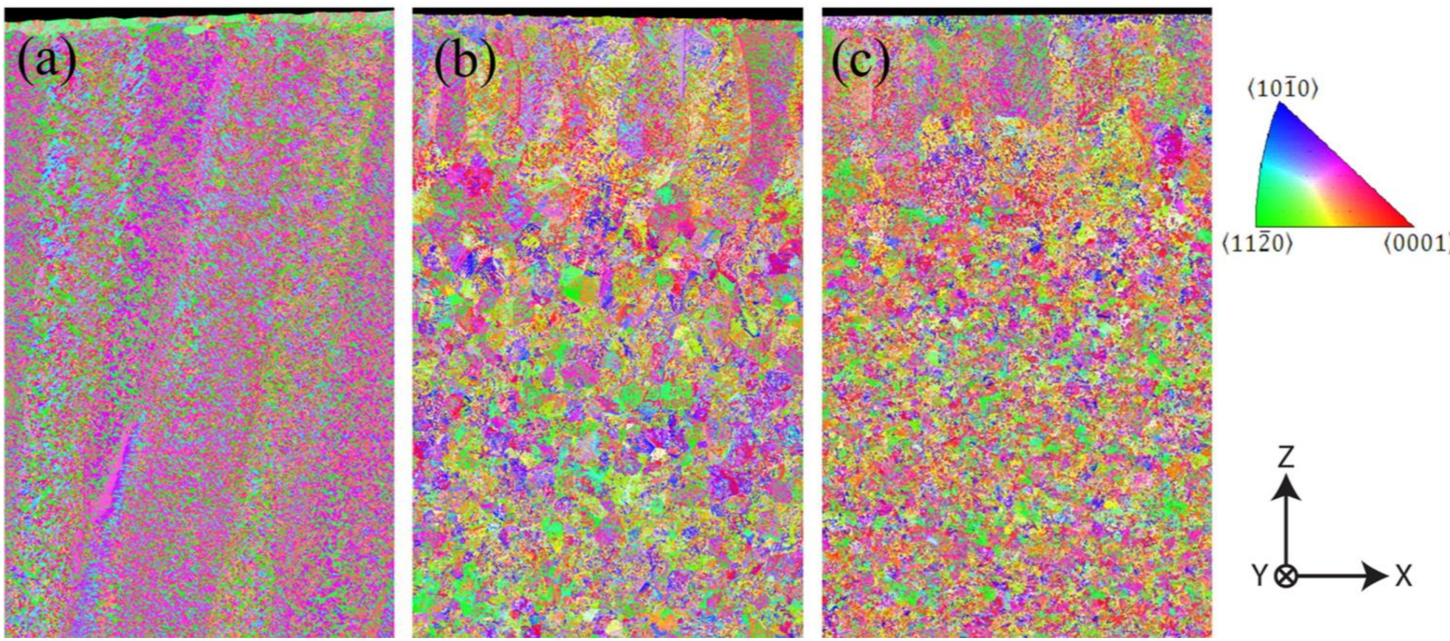

no rolling load | rolling load: 50kN | rolling load: 75kN

Donoghue, J., et al. "The effectiveness of combining rolling deformation with Wire–Arc Additive Manufacture on β-grain refinement and texture modification in Ti–6Al–4V." *Materials Characterization* 114 (2016): 103-114.

Ti64 – WAAM

Hybrid manufacturing: combining rolling and AM

Reconstructed parent β phase

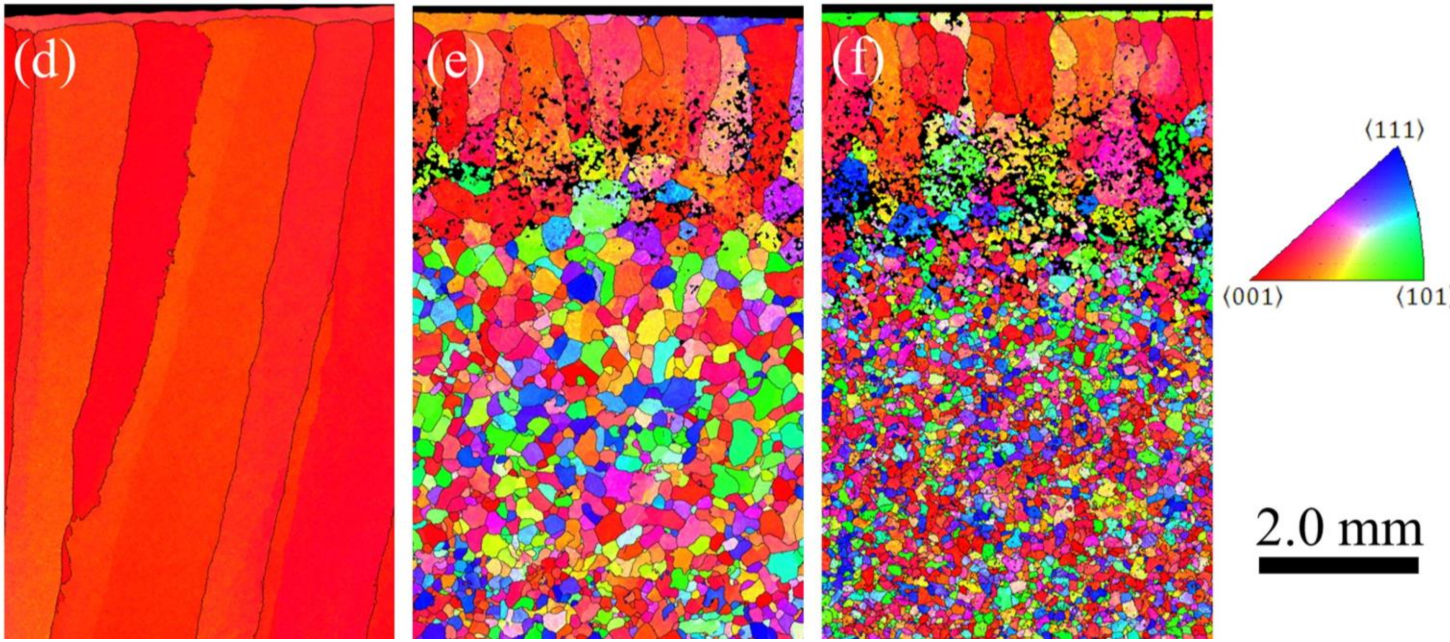

no rolling load | rolling load: 50kN | rolling load: 75kN

LONG COLUMNAR GRAINS

RECRYSTALLIZATION OF THE β GRAINS

Donoghue, J., et al. "The effectiveness of combining rolling deformation with Wire–Arc Additive Manufacture on β-grain refinement and texture modification in Ti–6Al–4V." *Materials Characterization* 114 (2016): 103-114.

Hybrid manufacturing: combining rolling and AM

Reconstructed parent β phase – {100} pole figures

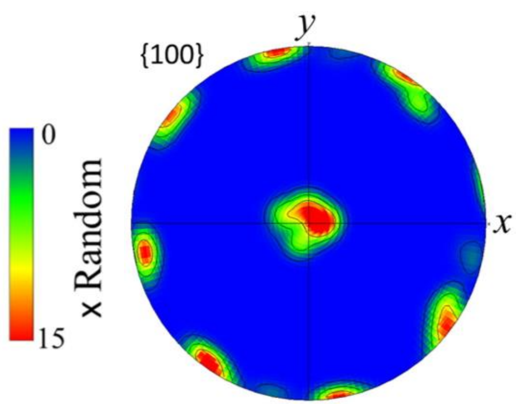

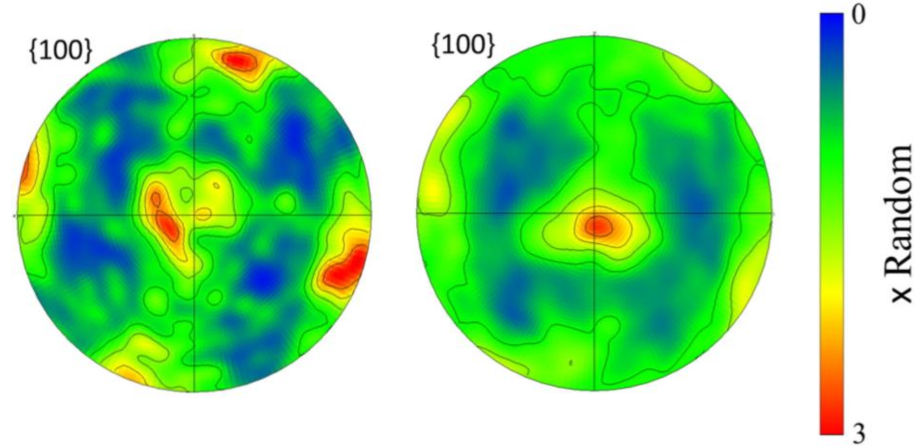

no rolling load

rolling load: 50kN rolling load: 75kN

STRONG <100>$_{\beta}$ FIBRE TEXTURE

WEAK TEXTURE, WITH SOME RESIDUAL <100> $_{\beta}$ FIBRE ORIENTATIONS

Donoghue, J., et al. "The effectiveness of combining rolling deformation with Wire–Arc Additive Manufacture on β-grain refinement and texture modification in Ti–6Al–4V." *Materials Characterization* 114 (2016): 103-114.

Hybrid manufacturing: combining rolling and AM

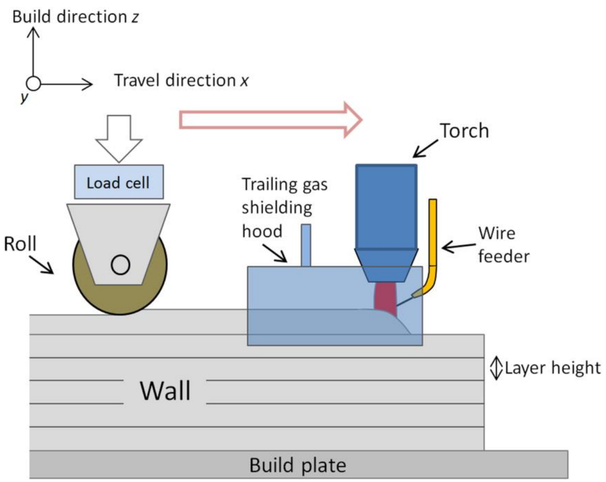

Rolling + WAAM is a useful technique for refining undesirable grain structures and reducing the intensity of the strong textures normally seen in the as-deposited material.
The compressive strain required to achieve a high level of β refinement is relatively low (19%), which makes it possible to apply this technology when producing simple geometries.

For more complex designs, other methods for introducing plastic deformation in AM should be considered (e.g. peening).

Donoghue, J., et al. "The effectiveness of combining rolling deformation with Wire–Arc Additive Manufacture on β-grain refinement and texture modification in Ti–6Al–4V." *Materials Characterization* 114 (2016): 103-114.

Microstructure control through processing

- Introduction: effect of thermal history on microstructure genesis
- Effect of scanning strategy
  - Effect of scanning direction
  - Effect of scanning length
- Effect of process parameters
- Effect of build geometry
- Effect of beamshaping
- Hybrid manufacturing
  - WAAM + rolling
  - LPBF + LSP

Hybrid manufacturing: combining LSP and AM

LPBF processing and stored (dislocation) energy

Normalized enthalpy vs normalized melt pool depth

$$\Delta H = \left(\frac{aP}{\sqrt{\pi\sigma^3 V\alpha}}\right) \qquad \Delta h = \rho(C_p\Delta T + L_m)$$

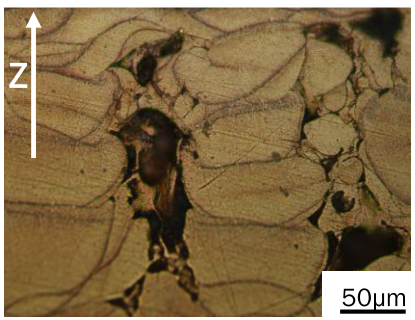

Lack of fusion (LoF)

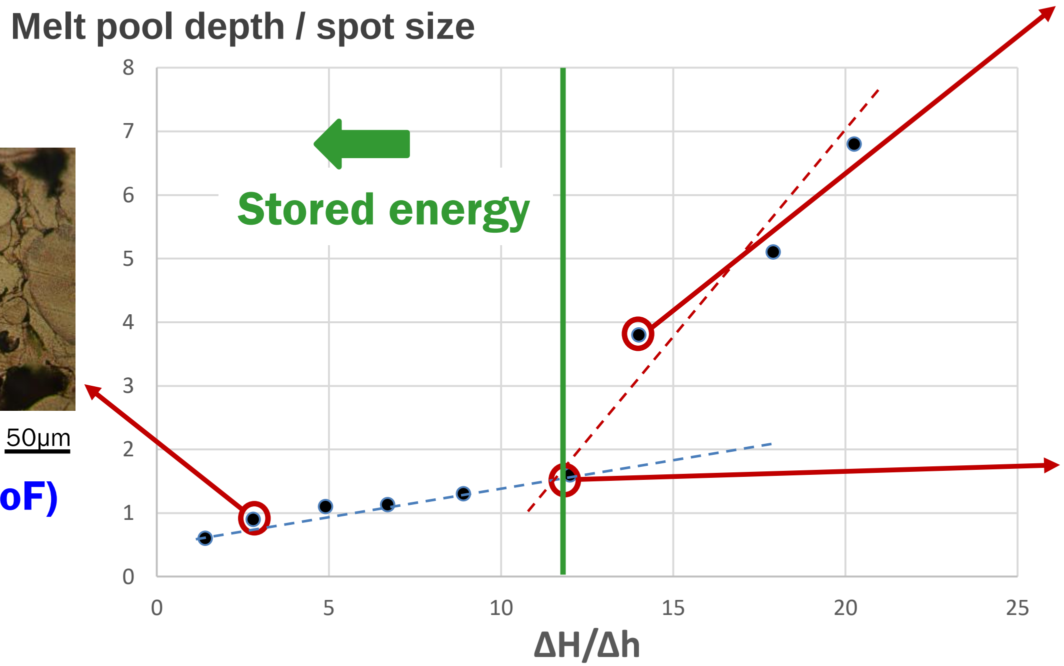

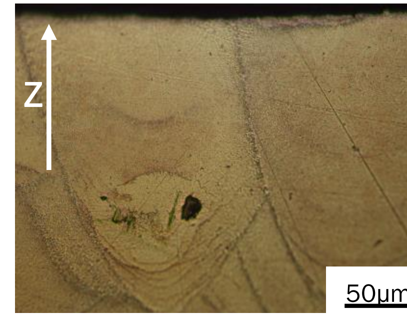

Keyhole porosities
Deep melt pool

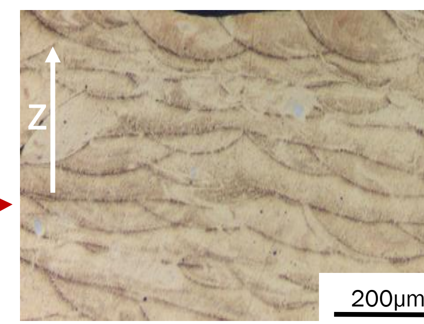

No Keyhole, No LoF
Conduction mode

Stored energy increases when approaching LoF
(reduced amount of heat, large thermal gradients)

316L – LPBF

Hybrid manufacturing: combining LSP and AM

Selective recrystallization by Laser Shock Peening (LSP)

<u>Case 1</u>: high stored energy, presence of porosities

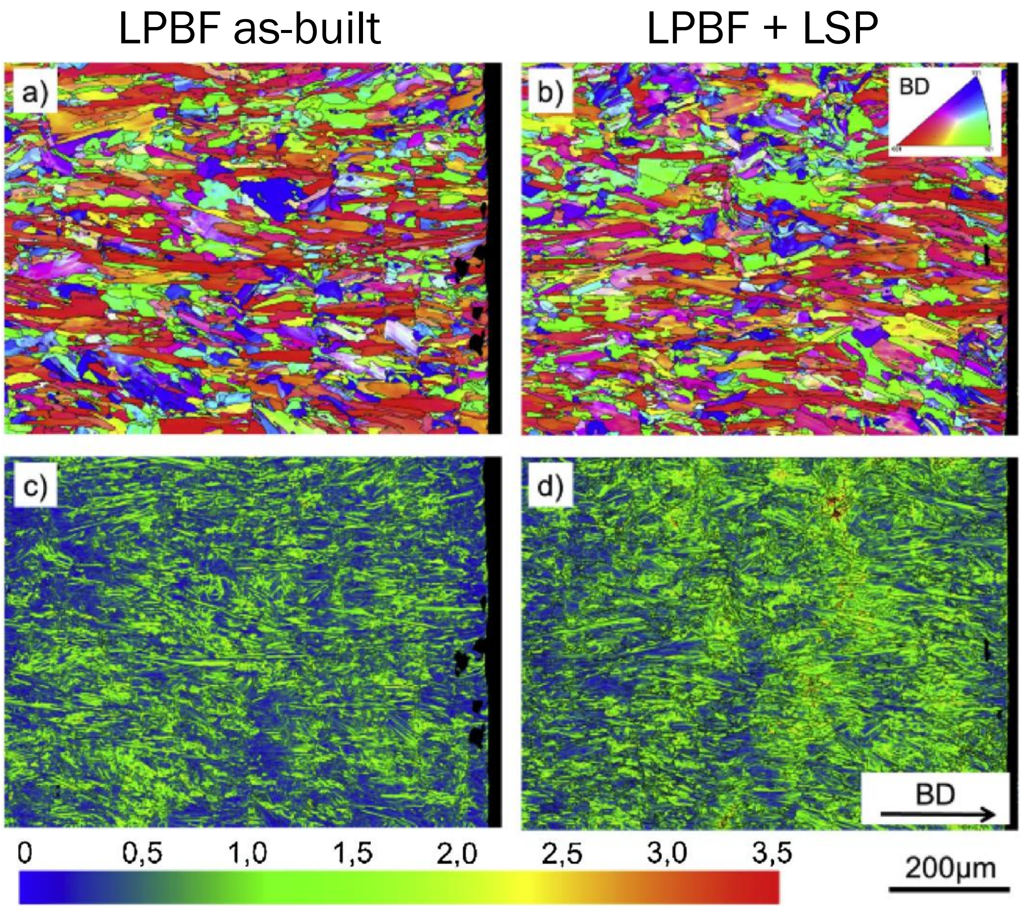

Inverse pole figure

Local misorientation

Kalentics, Nikola, et al. "Laser shock peening: A promising tool for tailoring metallic microstructures in selective laser melting." *Journal of Materials Processing Technology* 266 (2019): 612-618.

316L – LPBF

Hybrid manufacturing: combining LSP and AM

Selective recrystallization by Laser Shock Peening (LSP)

Case 1: high stored energy, presence of porosities

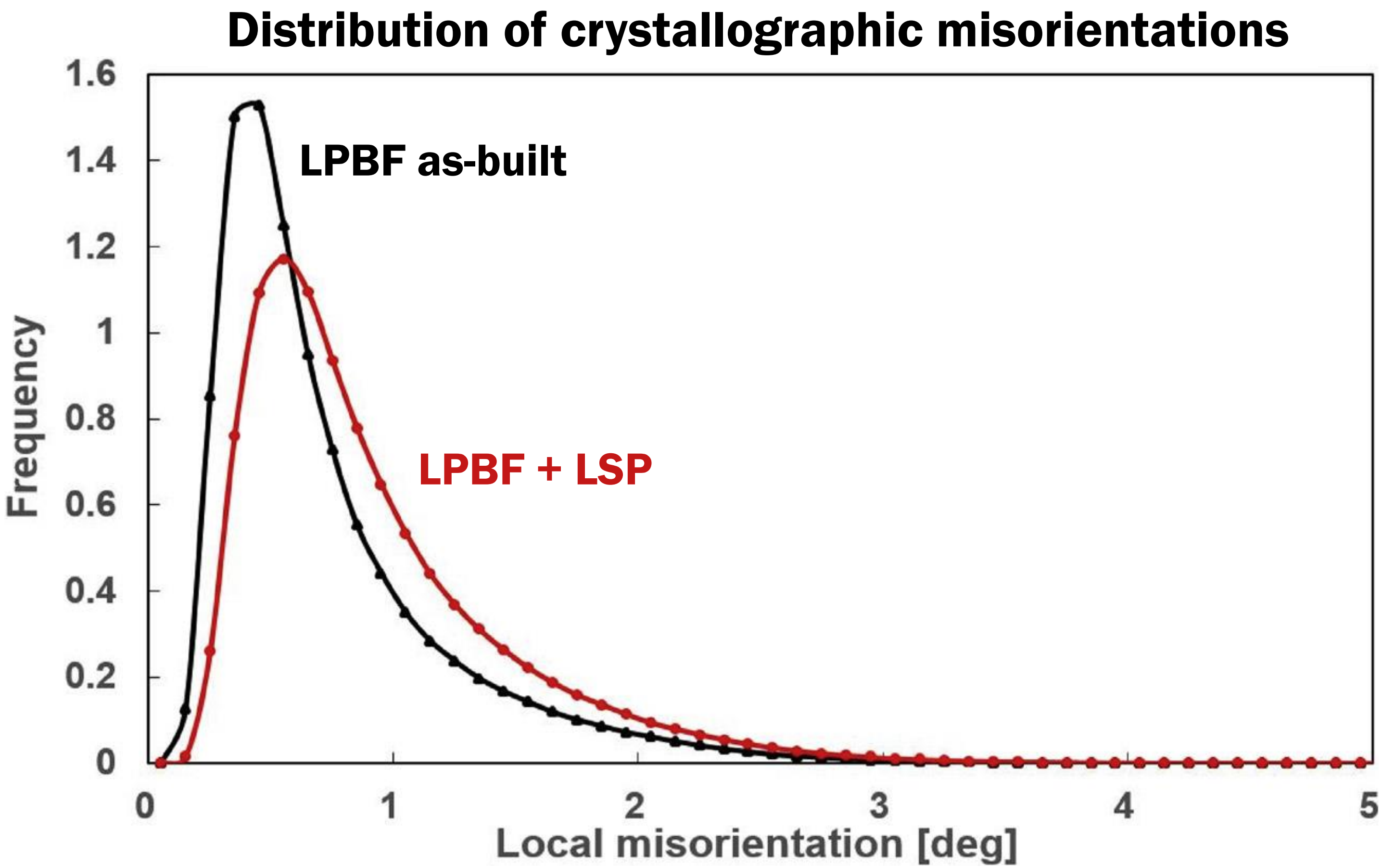

Kalentics et al., JMPT 2019

Hybrid manufacturing: combining LSP and AM

Selective recrystallization by Laser Shock Peening (LSP)

Case 1: high stored energy, presence of porosities

Heat treatment: 1100 °C – 10 min

LPBF as-built LPBF + LSP

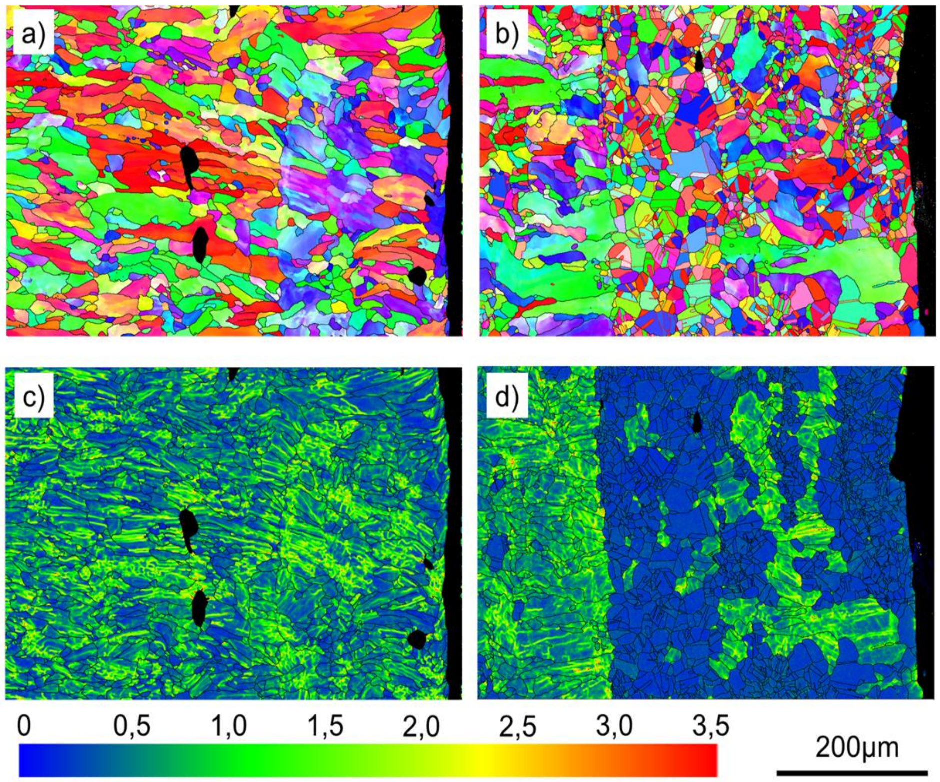

Inverse pole figure

Local misorientation

BD →

Kalentics, Nikola, et al. "Laser shock peening: A promising tool for tailoring metallic microstructures in selective laser melting." *Journal of Materials Processing Technology* 266 (2019): 612-618.

Hybrid manufacturing: combining LSP and AM

Selective recrystallization by Laser Shock Peening (LSP)

Case 1: high stored energy, presence of porosities

LPBF as-built annealed for 2 hours at 1100 °C does recrystallize

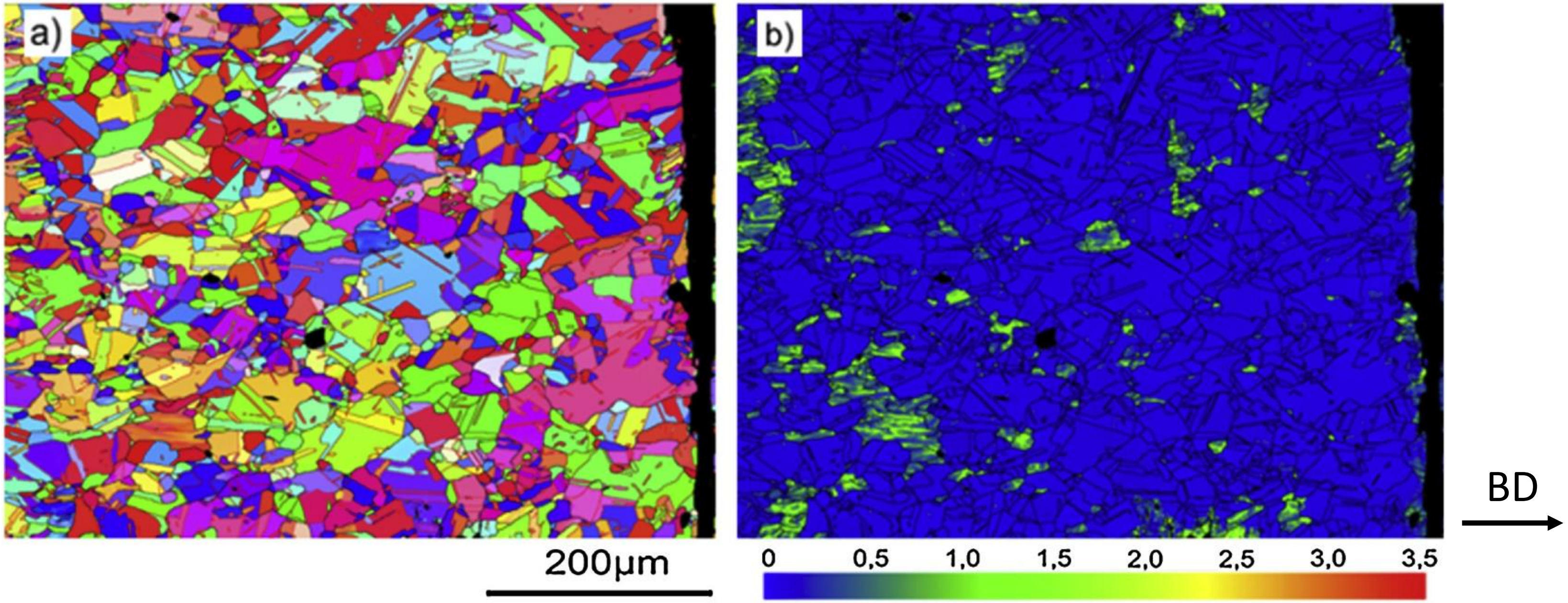

(Selective) LSP treatment accelerates REX kinetics
REX happens (slowly) without LSP due to the high SLM stored energy

Kalentics, Nikola, et al. "Laser shock peening: A promising tool for tailoring metallic microstructures in selective laser melting." *Journal of Materials Processing Technology* 266 (2019): 612-618.

Hybrid manufacturing: combining LSP and AM

Selective recrystallization by Laser Shock Peening (LSP)

Case 2: low stored energy, low porosity

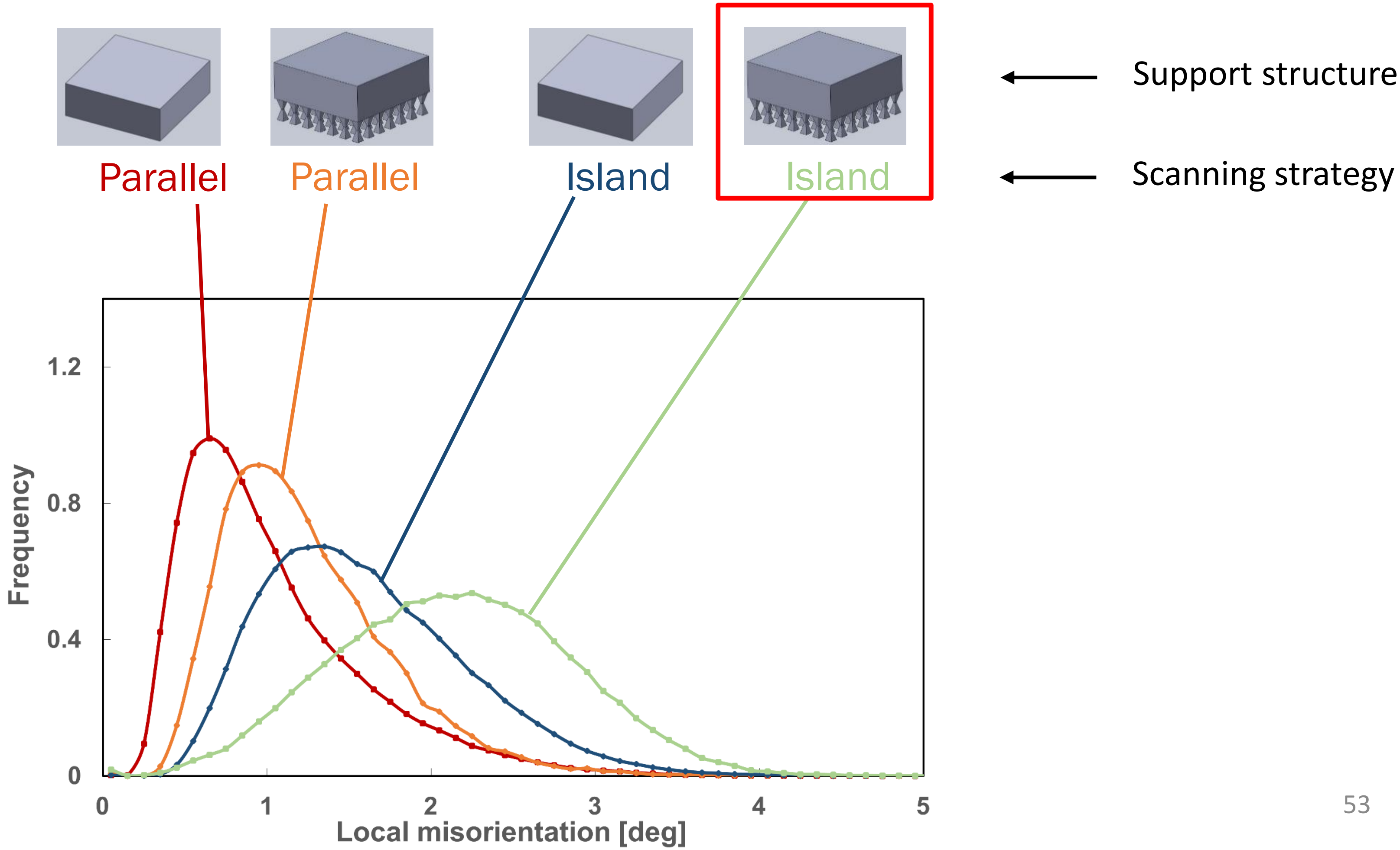

Hybrid manufacturing: combining LSP and AM

316L – LPBF

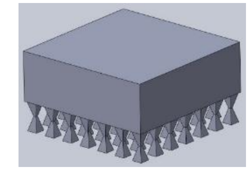

Island

Selective recrystallization by Laser Shock Peening (LSP)

Case 2: low stored energy, low porosity

As-built | **Heat treatment: 1100°C – 3h**

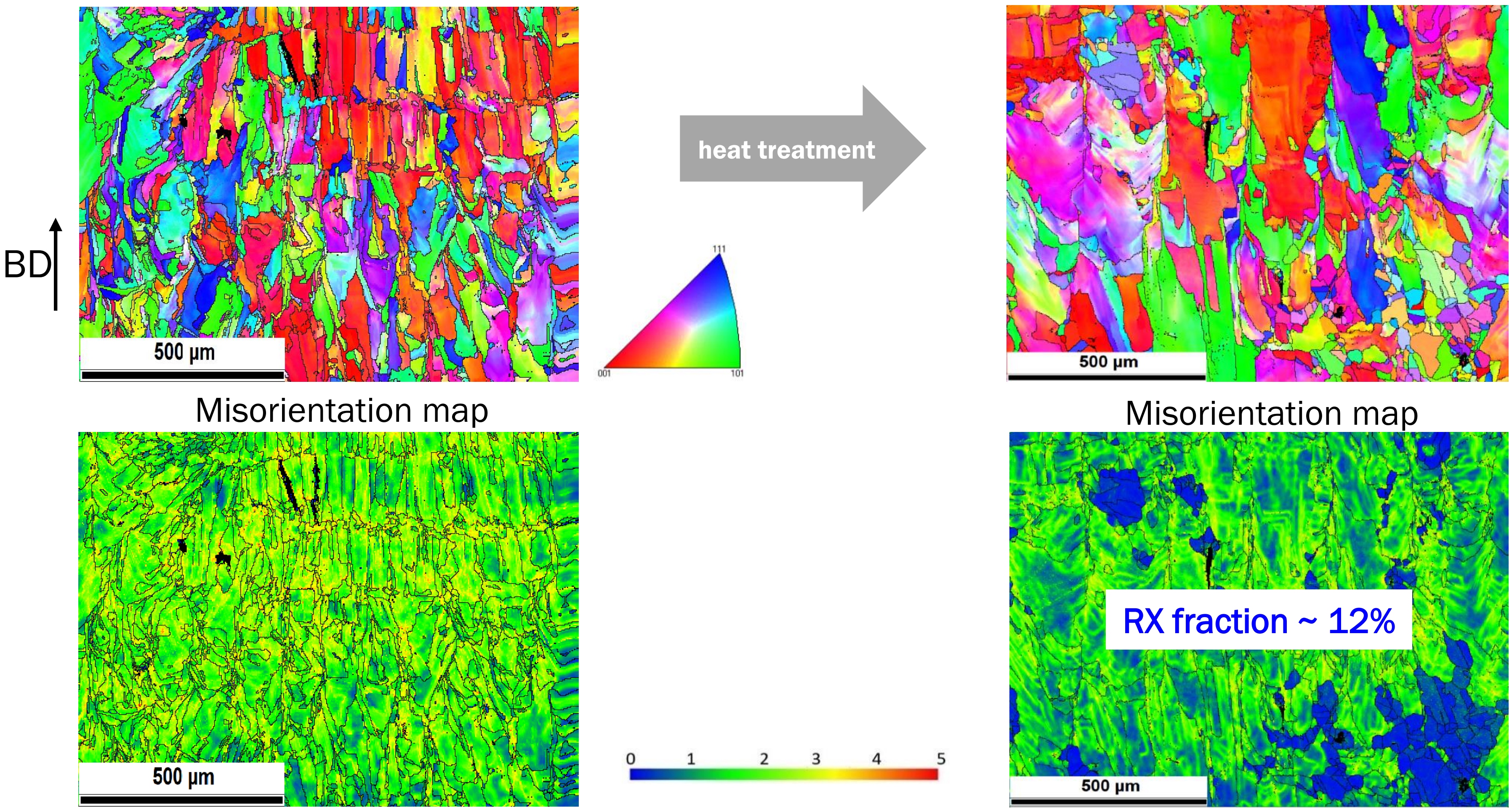

Hybrid manufacturing: combining LSP and AM

Selective recrystallization by Laser Shock Peening (LSP)

Case 2: low stored energy, low porosity

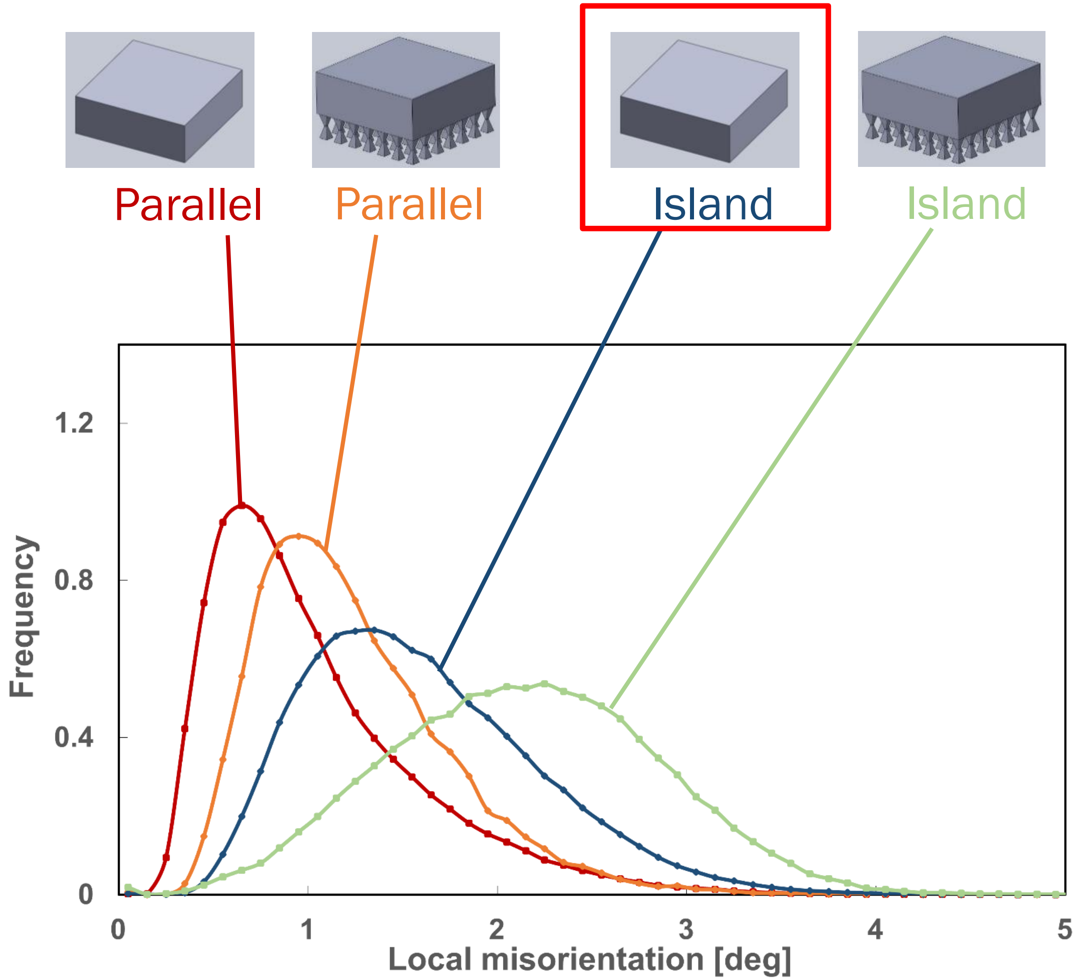

316L – LPBF

Hybrid manufacturing: combining LSP and AM

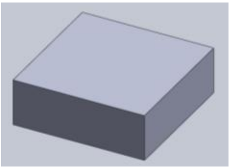

Island

Selective recrystallization by Laser Shock Peening (LSP)

Case 2: low stored energy, low porosity

LPBF + Heat treatment: 1100°C – 1h

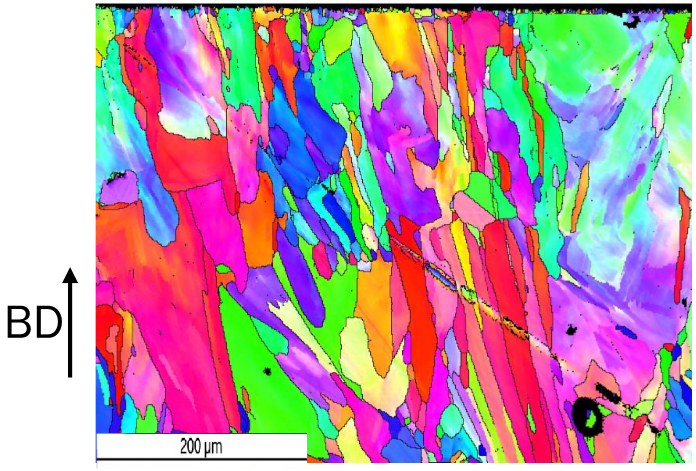

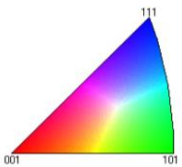

Misorientation map

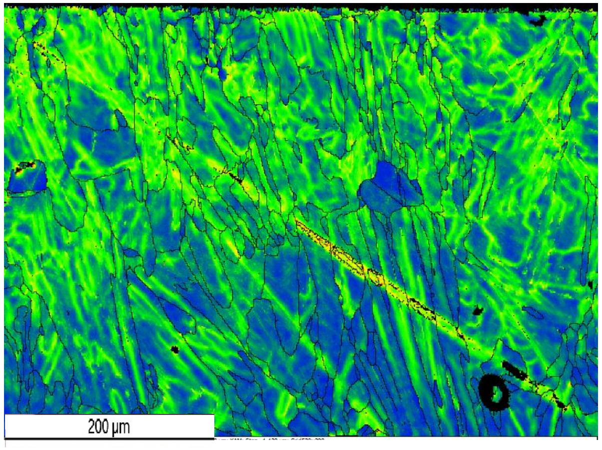

LPBF + LSP + Heat treatment: 1100°C – 1h

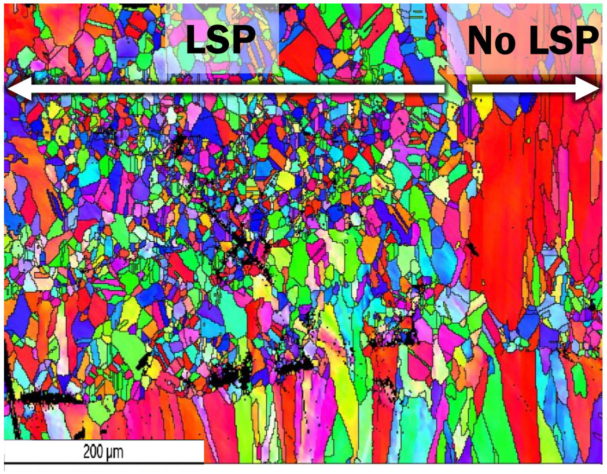

Misorientation map

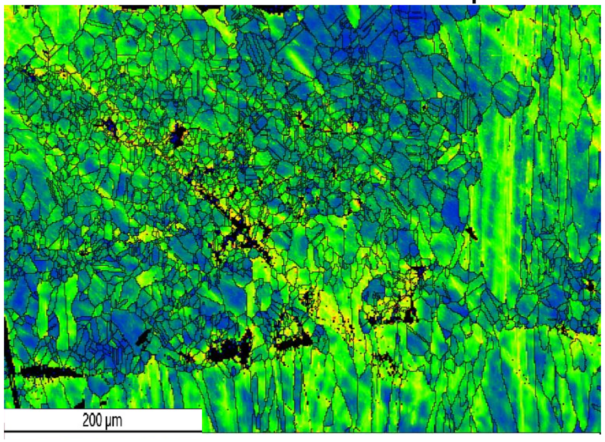

Hybrid manufacturing: combining LSP and AM

3D LSP: LSP combined with LPBF (chap. 5)

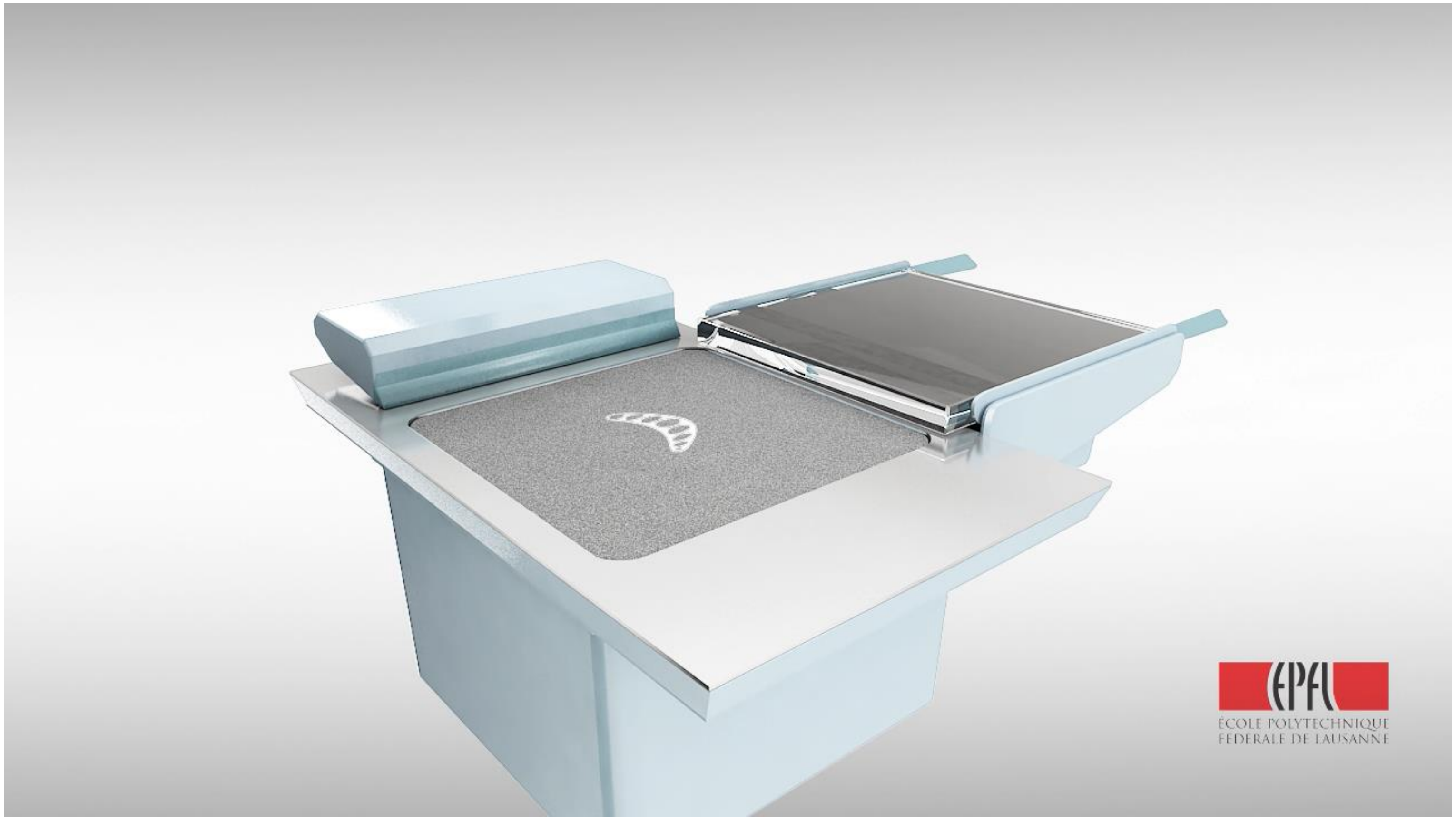

2D LSP treatment is applied periodically during the LPBF layer-by-layer building of the 3D piece, leading to 3D LSP **[EPFL patented]**

Hybrid manufacturing: combining LSP and AM

Strategy for healing cracks (chap. 5) → tailored recrystallization in 3D

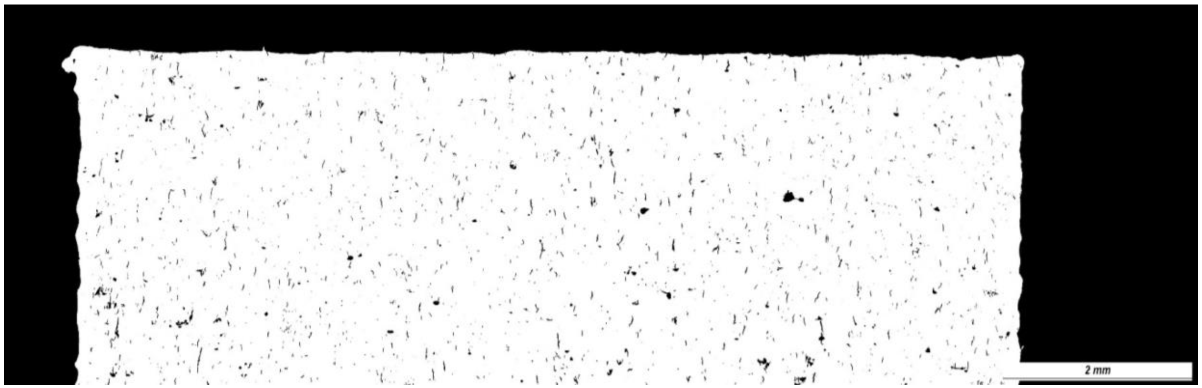

As-built sample

Zone with reduced crack density → zone of recrystallized grains

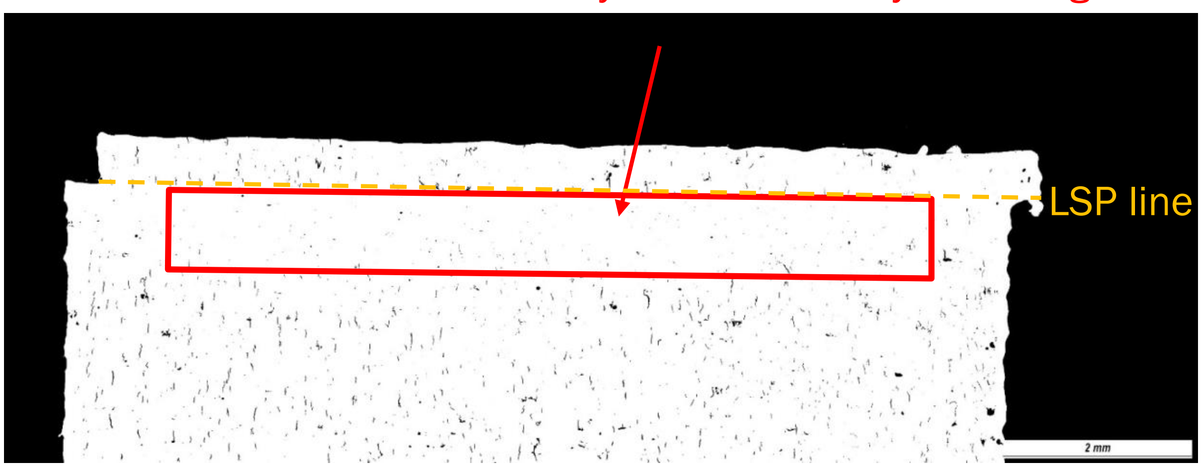

LSP
+
20 SLM layers on top

Kalentics, Nikola, et al. "Healing cracks in selective laser melting by 3D laser shock peening." *Additive Manufacturing* 30 (2019): 100881.